A Direct Arbitrary-Lagrangian-Eulerian ADER-WENO Finite Volume Scheme on Unstructured Tetrahedral Meshes for Conservative and Nonconservative Hyperbolic Systems in 3D

Walter Boscheri and Michael Dumbser
walter.boscheri@unitn.it

University of Trento (Italy)
- Department of Civil, Environmental and Mechanical Engineering -

SHARK FV 2015
May, 18^{th} – 22^{nd} 2015 - Ofir

European Research Council
erc

Outline

1. Introduction
2. Numerical Method
   - Hyperbolic Balance Laws
   - High Order WENO Reconstruction on Unstructured Meshes
   - Local Space-Time DG Predictor on Moving Meshes
   - Mesh Motion
   - Solution Algorithm
3. Validation
   - The Euler equations
   - The Baer–Nunziato Model
4. Conclusions and Outlook

Introduction: Lagrangian methods

$$\frac{D}{Dt}() = \frac{\partial}{\partial t}() + \overline{\mathbf{v}}\,\nabla()$$

Advantages

- availability of trajectory information;
- no convection terms $\rightarrow$ numerical stability;
- less numerical diffusion;
- material interfaces are precisely located and identified.

Introduction: Lagrangian methods

$$\frac{D}{Dt}() = \frac{\partial}{\partial t}() + \overline{\mathbf{v}}\,\nabla()$$

Advantages

- availability of trajectory information;
- no convection terms $\rightarrow$ numerical stability;
- less numerical diffusion;
- material interfaces are precisely located and identified.

Disadvantages

- high computational cost;
- mesh distortion.

Outline

1. Introduction
2. Numerical Method
   - Hyperbolic Balance Laws
   - High Order WENO Reconstruction on Unstructured Meshes
   - Local Space-Time DG Predictor on Moving Meshes
   - Mesh Motion
   - Solution Algorithm
3. Validation
   - The Euler equations
   - The Baer–Nunziato Model
4. Conclusions and Outlook

Hyperbolic Balance Laws

$$\frac{\partial \mathbf{Q}}{\partial t} + \nabla \cdot \mathbf{F}(\mathbf{Q}) + \mathbf{B}(\mathbf{Q}) \cdot \nabla \mathbf{Q} = \mathbf{S}(\mathbf{Q}), \qquad \mathbf{x} \in \Omega \subset \mathbb{R}^3, t \in \mathbb{R}_0^+ \qquad (1)$$

where

$\mathbf{Q} \in \Omega_Q \subset \mathbb{R}^\nu$ $\rightarrow$ state vector

$\mathbf{F} = (\mathbf{f}, \mathbf{g}, \mathbf{h})$ $\rightarrow$ flux tensor (purely conservative part of (1))

$\mathbf{B} = (\mathbf{B}_1, \mathbf{B}_2, \mathbf{B}_3)$ $\rightarrow$ non–conservative terms of (1)

$\mathbf{S}(\mathbf{Q})$ $\rightarrow$ vector of algebraic source terms

$\mathbf{P}(\mathbf{Q}) = \mathbf{B}(\mathbf{Q}) \cdot \nabla \mathbf{Q}$ $\rightarrow$ abbreviation

Hyperbolic Balance Laws

Moving mesh

$$\mathcal{T}_\Omega^n = \bigcup_{i=1}^{N_E} T_i^n$$

$$k = 1,2,3,4 \qquad \forall T_i^n$$

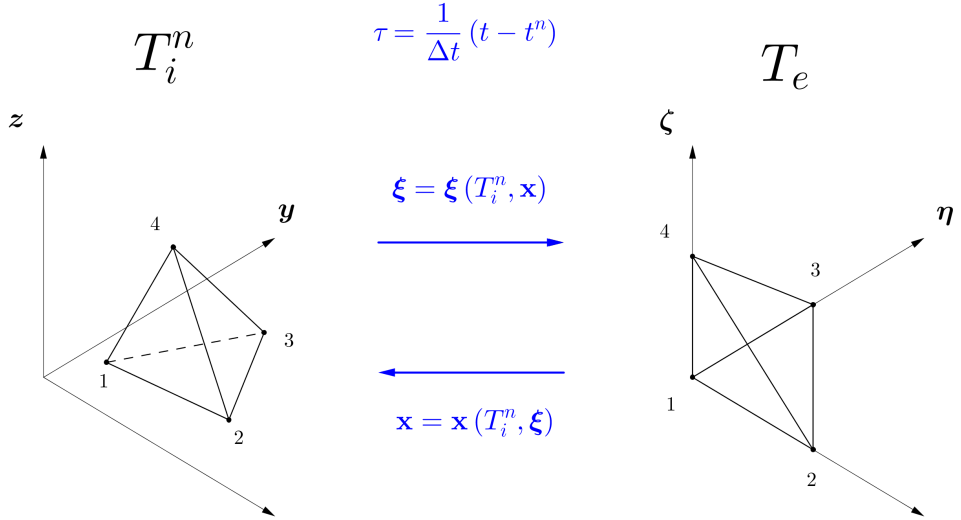

$$\begin{aligned} \mathbf{x} &= (x, y, z) \\ \boldsymbol{\xi} &= (\xi, \eta, \zeta) \end{aligned}$$

$$\begin{aligned} x &= X_{1,i}^n + \left(X_{2,i}^n - X_{1,i}^n\right)\xi + \left(X_{3,i}^n - X_{1,i}^n\right)\eta + \left(X_{4,i}^n - X_{1,i}^n\right)\zeta \\ y &= Y_{1,i}^n + \left(Y_{2,i}^n - Y_{1,i}^n\right)\xi + \left(Y_{3,i}^n - Y_{1,i}^n\right)\eta + \left(Y_{4,i}^n - Y_{1,i}^n\right)\zeta \\ z &= Z_{1,i}^n + \left(Z_{2,i}^n - Z_{1,i}^n\right)\xi + \left(Z_{3,i}^n - Z_{1,i}^n\right)\eta + \left(Z_{4,i}^n - Z_{1,i}^n\right)\zeta \end{aligned}$$

Hyperbolic Balance Laws

Moving mesh

$$\mathcal{T}_\Omega^n = \bigcup_{i=1}^{N_E} T_i^n$$

$$k = 1,2,3,4 \qquad \forall T_i^n$$

$$\begin{aligned} \mathbf{x} &= (x, y, z) \\ \boldsymbol{\xi} &= (\xi, \eta, \zeta) \end{aligned}$$

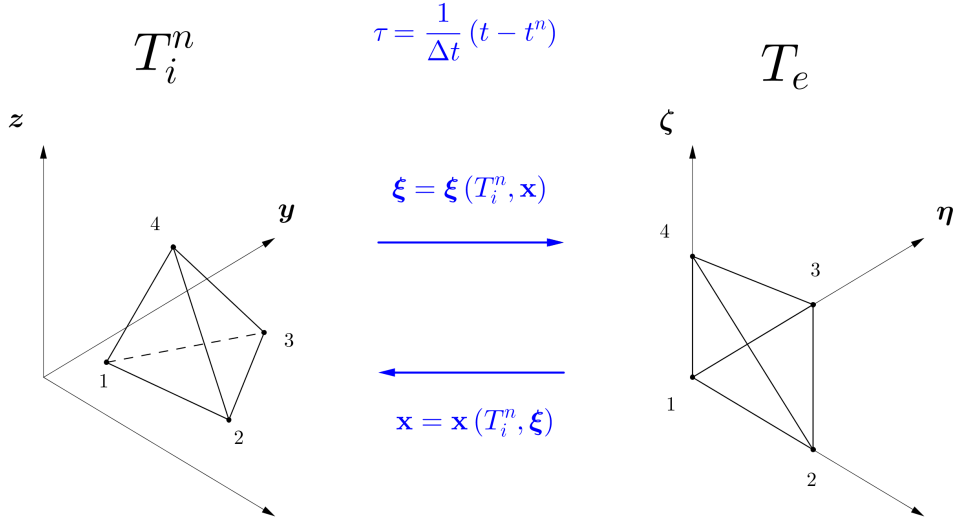

Data representation

$$\mathbf{Q}_i^n = \frac{1}{|T_i^n|} \int_{T_i^n} \mathbf{Q}(x, y, z, t^n) dV$$

Outline

1. Introduction
2. Numerical Method
   - Hyperbolic Balance Laws
   - High Order WENO Reconstruction on Unstructured Meshes
   - Local Space-Time DG Predictor on Moving Meshes
   - Mesh Motion
   - Solution Algorithm
3. Validation
   - The Euler equations
   - The Baer–Nunziato Model
4. Conclusions and Outlook

High Order of Accuracy in Space

Some spatial basis functions $\psi_l(\xi,\eta,\zeta)$ are used to write the reconstructed polynomials $\mathbf{w}_h^s$ for each reconstruction stencil s:

$$\mathbf{w}_h^s(x,y,z,t^n) = \sum_{l=1}^{\mathcal{M}} \psi_l(\xi,\eta,\zeta)\hat{\mathbf{w}}_{l,i}^{n,s} := \psi_l(\xi,\eta,\zeta)\hat{\mathbf{w}}_{l,i}^{n,s}$$

Integral conservation

$$\frac{1}{|T_j^n|}\int_{T_j^n} \psi_l(\xi,\eta,\zeta)\hat{\mathbf{w}}_{l,i}^{n,s}\,dV = \mathbf{Q}_j^n, \qquad \forall T_j^n \in \mathcal{S}_i^s$$

$$\begin{aligned} \mathcal{S}_i^s &= \bigcup_{j=1}^{n_e} T_{m(j)}^n \\ \mathcal{M} &= (M+1)(M+2)(M+3)/6 \\ n_e &= 3\mathcal{M} \end{aligned}$$

High Order of Accuracy in Space

Some spatial basis functions $\psi_l(\xi,\eta,\zeta)$ are used to write the reconstructed polynomials $\mathbf{w}_h^s$ for each reconstruction stencil s:

$$\mathbf{w}_h^s(x,y,z,t^n) = \sum_{l=1}^{\mathcal{M}} \psi_l(\xi,\eta,\zeta)\hat{\mathbf{w}}_{l,i}^{n,s} := \psi_l(\xi,\eta,\zeta)\hat{\mathbf{w}}_{l,i}^{n,s}$$

Integral conservation

$$\frac{1}{|T_j^n|}\int_{T_j^n} \psi_l(\xi,\eta,\zeta)\hat{\mathbf{w}}_{l,i}^{n,s}\,dV = \mathbf{Q}_j^n, \qquad \forall T_j^n \in \mathcal{S}_i^s$$

$$\begin{aligned} \mathcal{S}_i^s &= \bigcup_{j=1}^{n_e} T_{m(j)}^n \\ \mathcal{M} &= (M+1)(M+2)(M+3)/6 \\ n_e &= 3\mathcal{M} \end{aligned}$$

WENO polynomials

$$\mathbf{w}_h(x,y,z,t^n) = \sum_{l=1}^{\mathcal{M}} \psi_l(\xi,\eta,\zeta)\hat{\mathbf{w}}_{l,i}^{n}, \qquad \text{with} \qquad \hat{\mathbf{w}}_{l,i}^{n} = \sum_s \omega_s \hat{\mathbf{w}}_{l,i}^{n,s}$$

nonlinear WENO weights

$$\tilde{\omega}_s = \frac{\lambda_s}{(\sigma_s+\epsilon)^r}, \qquad \omega_s = \frac{\tilde{\omega}_s}{\sum_q \tilde{\omega}_q}$$

oscillation indicators

$$\sigma_s = \left(\sum_{\alpha+\beta+\gamma \le M} \int_{T_e} \frac{\partial^{\alpha+\beta+\gamma}\psi_l(\xi,\eta,\zeta)}{\partial\xi^\alpha\partial\eta^\beta\partial\zeta^\gamma} \cdot \frac{\partial^{\alpha+\beta+\gamma}\psi_m(\xi,\eta,\zeta)}{\partial\xi^\alpha\partial\eta^\beta\partial\zeta^\gamma} d\xi d\eta d\zeta \right)$$

Outline

1. Introduction
2. Numerical Method
   - Hyperbolic Balance Laws
   - High Order WENO Reconstruction on Unstructured Meshes
   - Local Space-Time DG Predictor on Moving Meshes
   - Mesh Motion
   - Solution Algorithm
3. Validation
   - The Euler equations
   - The Baer–Nunziato Model
4. Conclusions and Outlook

High Order of Accuracy in Time

$\tilde{\mathbf{x}} = (x, y, z, t)$ $\quad$ $\tilde{\boldsymbol{\xi}} = (\xi, \eta, \zeta, \tau)$ $\quad$ $\theta_l = \theta_l(\tilde{\boldsymbol{\xi}}) = \theta_l(\xi, \eta, \zeta, \tau)$

$\mathbf{x} = (x, y, z)$ $\quad$ $\boldsymbol{\xi} = (\xi, \eta, \zeta)$

physical coordinates $\quad$ reference coordinates $\quad$ space–time basis functions

Isoparametric approach

$$\mathbf{q}_h = \mathbf{q}_h(\xi, \eta, \zeta, \tau) = \theta_l(\xi, \eta, \zeta, \tau)\widehat{\mathbf{q}}_{l,i} \qquad \mathbf{F}_h = (\mathbf{f}_h, \mathbf{g}_h, \mathbf{h}_h) = \mathbf{F}_h(\xi, \eta, \zeta, \tau) = \theta_l(\xi, \eta, \zeta, \tau)\widehat{\mathbf{F}}_{l,i}$$

$$\mathbf{P}_h = \mathbf{B}(\mathbf{q}_h) \cdot \nabla \mathbf{q}_h = \mathbf{P}_h(\tilde{\boldsymbol{\xi}}) = \theta_l(\tilde{\boldsymbol{\xi}})\, \widehat{\mathbf{P}}_{l,i} \qquad \mathbf{S}_h = \mathbf{S}_h(\xi, \eta, \zeta, \tau) = \theta_l(\xi, \eta, \zeta, \tau)\widehat{\mathbf{S}}_{l,i}$$

$$\Downarrow$$

$$x(\xi, \eta, \zeta, \tau) = \theta_l(\xi, \eta, \zeta, \tau)\widehat{x}_{l,i}, \qquad y(\xi, \eta, \zeta, \tau) = \theta_l(\xi, \eta, \zeta, \tau)\widehat{y}_{l,i}$$
$$z(\xi, \eta, \zeta, \tau) = \theta_l(\xi, \eta, \zeta, \tau)\widehat{z}_{l,i}, \qquad t(\xi, \eta, \zeta, \tau) = \theta_l(\xi, \eta, \zeta, \tau)\widehat{t}_l$$

Jacobian

$$J_{st} = \frac{\partial \tilde{\mathbf{x}}}{\partial \tilde{\boldsymbol{\xi}}} = \begin{pmatrix} x_\xi & x_\eta & x_\zeta & x_\tau \\ y_\xi & y_\eta & y_\zeta & y_\tau \\ z_\xi & z_\eta & z_\zeta & z_\tau \\ 0 & 0 & 0 & \Delta t \end{pmatrix} \qquad J_{st}^{-1} = \frac{\partial \tilde{\boldsymbol{\xi}}}{\partial \tilde{\mathbf{x}}} = \begin{pmatrix} \xi_x & \xi_y & \xi_z & \xi_t \\ \eta_x & \eta_y & \eta_z & \eta_t \\ \zeta_x & \zeta_y & \zeta_z & \zeta_t \\ 0 & 0 & 0 & \frac{1}{\Delta t} \end{pmatrix}$$

High Order of Accuracy in Time

The PDE in the reference coordinate system

$$\nabla_{\boldsymbol{\xi}} = \begin{pmatrix} \frac{\partial}{\partial \xi} \\ \frac{\partial}{\partial \eta} \\ \frac{\partial}{\partial \zeta} \end{pmatrix}, \qquad \nabla = \begin{pmatrix} \frac{\partial}{\partial x} \\ \frac{\partial}{\partial y} \\ \frac{\partial}{\partial z} \end{pmatrix} = \begin{pmatrix} \xi_x & \eta_x & \zeta_x \\ \xi_y & \eta_y & \zeta_y \\ \xi_z & \eta_z & \zeta_z \end{pmatrix} \begin{pmatrix} \frac{\partial}{\partial \xi} \\ \frac{\partial}{\partial \eta} \\ \frac{\partial}{\partial \zeta} \end{pmatrix} = \left(\frac{\partial \boldsymbol{\xi}}{\partial \mathbf{x}} \right)^T \nabla_{\boldsymbol{\xi}}$$

$$\Downarrow$$

$$\frac{\partial \mathbf{Q}}{\partial \tau} + \Delta t \left[\frac{\partial \mathbf{Q}}{\partial \boldsymbol{\xi}} \cdot \frac{\partial \boldsymbol{\xi}}{\partial t} + \left(\frac{\partial \boldsymbol{\xi}}{\partial \mathbf{x}} \right)^T \nabla_{\boldsymbol{\xi}} \cdot \mathbf{F} + \mathbf{B}(\mathbf{Q}) \cdot \left(\frac{\partial \boldsymbol{\xi}}{\partial \mathbf{x}} \right)^T \nabla_{\boldsymbol{\xi}} \mathbf{Q} \right] = \Delta t \mathbf{S}(\mathbf{Q})$$

Let define the following operators:

$$[f,g]^{\tau} = \int_{T_e} f(\xi,\eta,\zeta,\tau) g(\xi,\eta,\zeta,\tau) d\xi d\eta d\zeta, \qquad \langle f,g \rangle = \int_0^1 \int_{T_e} f(\xi,\eta,\zeta,\tau) g(\xi,\eta,\zeta,\tau) d\xi d\eta d\zeta d\tau.$$

High Order of Accuracy in Time

$$\frac{\partial \mathbf{Q}}{\partial \tau} = \Delta t \mathbf{H}$$

$$\mathbf{H} = \Delta t \mathbf{S} - \Delta t \left[\frac{\partial \mathbf{Q}}{\partial \boldsymbol{\xi}} \cdot \frac{\partial \boldsymbol{\xi}}{\partial t} + \left(\frac{\partial \boldsymbol{\xi}}{\partial \mathbf{x}} \right)^T \nabla_{\boldsymbol{\xi}} \cdot \mathbf{F} + \mathbf{B}(\mathbf{Q}) \cdot \left(\frac{\partial \boldsymbol{\xi}}{\partial \mathbf{x}} \right)^T \nabla_{\boldsymbol{\xi}} \mathbf{Q} \right], \quad \mathbf{H}_h = \theta_l(\tilde{\boldsymbol{\xi}}) \, \widehat{\mathbf{H}}_{l,i}.$$

Multiplication with $\theta_k(\boldsymbol{\xi})$ and integration over $T_e \times [0,1]$ yields the weak formulation of the PDE, i.e.

$$\left\langle \theta_k, \frac{\partial \theta_l}{\partial \tau} \right\rangle \widehat{\mathbf{q}}_{l,i} = \langle \theta_k, \theta_l \rangle \, \Delta t \, \widehat{\mathbf{H}}_{l,i}$$

High Order of Accuracy in Time

The nonlinear algebraic equation system can be written in a more compact matrix form as

$$K_1 \widehat{\mathbf{q}}_{l,i} = \mathbf{F}_0 \hat{\mathbf{w}}^n_{l,i} + \mathbf{M} \widehat{\mathbf{H}}_{l,i}$$

$$K_1 = [\theta_k(\boldsymbol{\xi}, 1), \theta_l(\boldsymbol{\xi}, 1)]^1 - \left\langle \frac{\partial \theta_k}{\partial \tau}, \theta_l \right\rangle, \quad \mathbf{F}_0 = [\theta_k(\boldsymbol{\xi}, 0), \psi_l(\boldsymbol{\xi})], \quad \mathbf{M} = \langle \theta_k, \theta_l \rangle .$$

High Order of Accuracy in Time

The nonlinear algebraic equation system can be written in a more compact matrix form as

$$K_1 \widehat{\mathbf{q}}_{l,i} = \mathbf{F}_0 \hat{\mathbf{w}}^n_{l,i} + \mathbf{M} \widehat{\mathbf{H}}_{l,i}$$

$$K_1 = [\theta_k(\boldsymbol{\xi}, 1), \theta_l(\boldsymbol{\xi}, 1)]^1 - \left\langle \frac{\partial \theta_k}{\partial \tau}, \theta_l \right\rangle, \quad \mathbf{F}_0 = [\theta_k(\boldsymbol{\xi}, 0), \psi_l(\boldsymbol{\xi})], \quad \mathbf{M} = \langle \theta_k, \theta_l \rangle .$$

local PDE evolution

$$\widehat{\mathbf{q}}^{r+1}_{l,i} = K_1^{-1} \left(\mathbf{F}_0 \hat{\mathbf{w}}^n_{l,i} + \mathbf{M} \widehat{\mathbf{H}}^r_{l,i} \right)$$

High Order of Accuracy in Time

The nonlinear algebraic equation system can be written in a more compact matrix form as

$$K_1 \widehat{\mathbf{q}}_{l,i} = \mathbf{F}_0 \hat{\mathbf{w}}^n_{l,i} + \mathbf{M}\widehat{\mathbf{H}}_{l,i}$$

$$K_1 = [\theta_k(\boldsymbol{\xi},1), \theta_l(\boldsymbol{\xi},1)]^1 - \left\langle \frac{\partial \theta_k}{\partial \tau}, \theta_l \right\rangle, \quad \mathbf{F}_0 = [\theta_k(\boldsymbol{\xi},0), \psi_l(\boldsymbol{\xi})], \quad \mathbf{M} = \langle \theta_k, \theta_l \rangle .$$

local PDE evolution

$$\hat{\mathbf{q}}^{r+1}_{l,i} = K_1^{-1} \left(\mathbf{F}_0 \hat{\mathbf{w}}^n_{l,i} + \mathbf{M}\widehat{\mathbf{H}}^r_{l,i} \right)$$

geometry evolution

$$\frac{d\mathbf{x}}{dt} = \mathbf{V}(\mathbf{Q}, \mathbf{x}, t) \qquad \mathbf{V}_h = \theta_l(\boldsymbol{\xi}, \tau)\widehat{\mathbf{V}}_{l,i}$$

$$\widehat{\mathbf{V}}_{l,i} = \mathbf{V}(\hat{\mathbf{q}}_{l,i}, \hat{\mathbf{x}}_{l,i}, \hat{t}_l)$$

$$K_1 \widehat{\mathbf{x}}_{l,i} = [\theta_k(\boldsymbol{\xi},0), \mathbf{x}(\boldsymbol{\xi}, t^n)]^0 + \Delta t \mathbf{M}\, \widehat{\mathbf{V}}_{l,i}$$

Outline

1. Introduction
2. Numerical Method
   - Hyperbolic Balance Laws
   - High Order WENO Reconstruction on Unstructured Meshes
   - Local Space-Time DG Predictor on Moving Meshes
   - Mesh Motion
   - Solution Algorithm
3. Validation
   - The Euler equations
   - The Baer–Nunziato Model
4. Conclusions and Outlook

Nodal solvers

1) The node solver of Cheng and Shu $\mathcal{NS}_{cs}$ (*JCP* 227: 1567-1596, 2007)

$$\overline{\mathbf{v}}_k^n = \frac{1}{\mu_k} \sum_{j \in \mathcal{V}_k} \overline{\mathbf{v}}_{k,j}^n \quad \text{with} \quad \overline{\mathbf{v}}_{k,j}^n = \left(\int_0^1 \theta_l(\xi_{e,m(k)}, \eta_{e,m(k)}, \zeta_{e,m(k)}, \tau) d\tau \right) \widehat{\mathbf{v}}_{l,j}$$

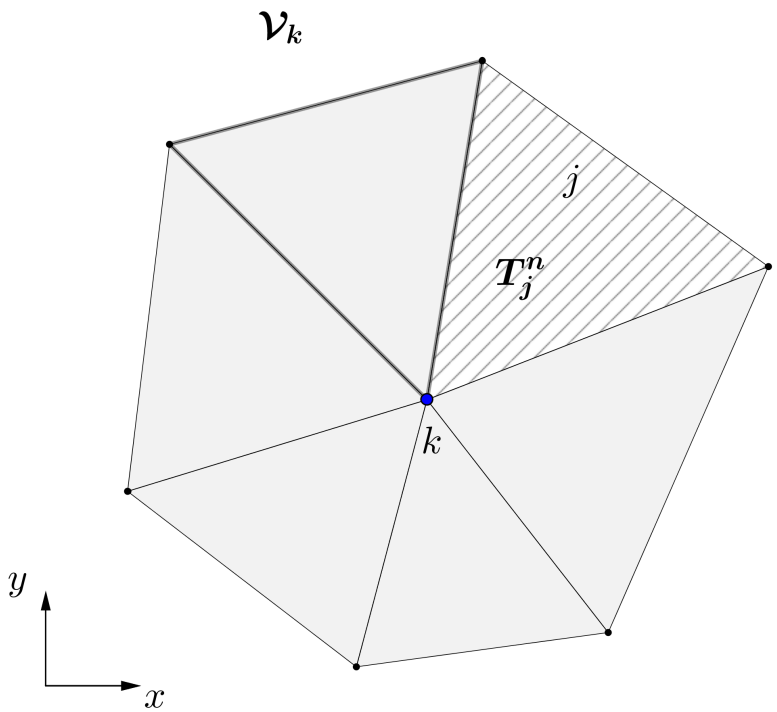

$$\mu_k = \sum_{T_j^n \in \mathcal{V}_k} 1 = N_k$$

or

$$\mu_k = \sum_{T_j^n \in \mathcal{V}_k} \mu_{k,j} \qquad \mu_{k,j} = \rho_j^n |T_j^n|$$

Nodal solvers

2) The node solver of Maire $\mathcal{NS}_m$ (*JCP* 228: 2391-2425, 2009)

$$\overline{\mathbf{V}}_k^n = M_k^{-1} \sum_{j \in \mathcal{V}_k} \left(L_{k,j} P_j \mathbf{n}_j + M_{p,j} \mathbf{V}_j \right)$$

with

$$M_{k,j} = \sum_{f \in j} Z_{k,f}^j L_{k,f}^j \left(\mathbf{n}_{k,f}^j \otimes \mathbf{n}_{k,f}^j \right), \quad M_k = \sum_{j \in \mathcal{V}_k} M_{k,j}, \quad Z_{k,f}^j = \rho_j c_j$$

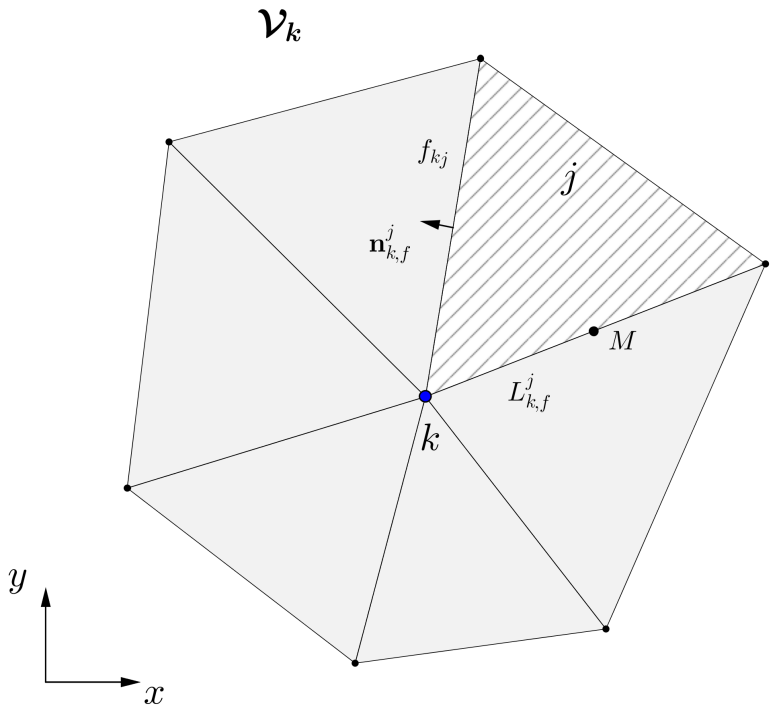

Geometry Evolution

- *Lagrangian coordinates*

$$\mathbf{x}_k^{n+1,Lag} = \mathbf{x}_k^n + \overline{\mathbf{V}}_k^n \cdot \Delta t$$

- *Rezoned coordinates*

$$F_k(\mathbf{x}_k) = \sum_{j \in \mathcal{V}_k} \mathcal{K}(\mathbf{J}_j), \quad \mathbf{J}_j = \begin{pmatrix} x_{k+3}^j - x_k^j & x_{k+2}^j - x_k^j & x_{k+1}^j - x_k^j \\ y_{k+3}^j - y_k^j & y_{k+2}^j - y_k^j & y_{k+1}^j - y_k^j \\ z_{k+3}^j - z_k^j & z_{k+2}^j - z_k^j & z_{k+1}^j - z_k^j \end{pmatrix}$$

$$\mathbf{x}_k^{rez} \quad \rightarrow \quad min\left\{F_k(\mathbf{x}_k)\right\}$$

- *New coordinates* (relaxation algorithm [1])

$$\mathbf{x}_k^{n+1} = \mathbf{x}_k^{n+1,Lag} + \omega_k \left(\mathbf{x}_k^{rez} - \mathbf{x}_k^{n+1,Lag}\right), \qquad \omega_k = \mathcal{F}\left(\mathbf{x}_k^n, \mathbf{x}_k^{n+1,Lag}\right)$$

[1] Galera et al., *JCP* 229: 5755-5787, 2010

Outline

1. Introduction
2. Numerical Method
   - Hyperbolic Balance Laws
   - High Order WENO Reconstruction on Unstructured Meshes
   - Local Space-Time DG Predictor on Moving Meshes
   - Mesh Motion
   - Solution Algorithm
3. Validation
   - The Euler equations
   - The Baer–Nunziato Model
4. Conclusions and Outlook

Finite Volume Scheme

The starting PDE system can be rewritten as

$$\tilde{\nabla} \cdot \tilde{\mathbf{F}} + \tilde{\mathbf{B}}(\mathbf{Q}) \cdot \tilde{\nabla}\mathbf{Q} = \mathbf{S}(\mathbf{Q})$$

with

$$\tilde{\nabla} = \left(\frac{\partial}{\partial x}, \frac{\partial}{\partial y}, \frac{\partial}{\partial z}, \frac{\partial}{\partial t} \right)^T, \qquad \tilde{\mathbf{F}} = (\mathbf{f}, \mathbf{g}, \mathbf{h}, \mathbf{Q}), \qquad \tilde{\mathbf{B}} = (\mathbf{B}_1, \mathbf{B}_2, \mathbf{B}_3).$$

Integration over the space–time control volume $\mathcal{C}_i^n = T_i(t) \times \left[t^n; t^{n+1}\right]$ yields

$$\int_{\mathcal{C}_i^n} \tilde{\nabla} \cdot \tilde{\mathbf{F}} \, d\mathbf{x}dt + \int_{\mathcal{C}_i^n} \tilde{\mathbf{B}}(\mathbf{Q}) \cdot \tilde{\nabla}\mathbf{Q} \, d\mathbf{x}dt = \int_{\mathcal{C}_i^n} \mathbf{S}(\mathbf{Q}) \, d\mathbf{x}dt$$

Finite Volume Scheme

Application of *Gauss' theorem* leads to

$$\int_{\partial \mathcal{C}_i^n} \left(\tilde{\mathbf{F}} + \tilde{\mathbf{D}} \right) \cdot \tilde{\mathbf{n}} \, dS + \int_{\mathcal{C}_i^n \setminus \partial \mathcal{C}_i^n} \tilde{\mathbf{B}}(\mathbf{Q}) \cdot \tilde{\nabla} \mathbf{Q} \, d\mathbf{x} dt = \int_{\mathcal{C}_i^n} \mathbf{S}(\mathbf{Q}) \, d\mathbf{x} dt$$

where

$$\tilde{\mathbf{n}} = (\tilde{n}_x, \tilde{n}_y, \tilde{n}_z, \tilde{n}_t), \qquad \tilde{\mathbf{D}} \cdot \tilde{\mathbf{n}} = \frac{1}{2} \int_0^1 \tilde{\mathbf{B}} \left(\boldsymbol{\Psi}(\mathbf{Q}^-, \mathbf{Q}^+, s) \right) \cdot \tilde{\mathbf{n}} \, \frac{\partial \boldsymbol{\Psi}}{\partial s} \, ds.$$

Finite Volume Scheme

Application of *Gauss' theorem* leads to

$$\int_{\partial \mathcal{C}_i^n} \left(\tilde{\mathbf{F}} + \tilde{\mathbf{D}} \right) \cdot \tilde{\mathbf{n}} \, dS + \int_{\mathcal{C}_i^n \setminus \partial \mathcal{C}_i^n} \tilde{\mathbf{B}}(\mathbf{Q}) \cdot \tilde{\nabla} \mathbf{Q} \, d\mathbf{x} dt = \int_{\mathcal{C}_i^n} \mathbf{S}(\mathbf{Q}) \, d\mathbf{x} dt$$

where

$$\tilde{\mathbf{n}} = (\tilde{n}_x, \tilde{n}_y, \tilde{n}_z, \tilde{n}_t), \qquad \tilde{\mathbf{D}} \cdot \tilde{\mathbf{n}} = \frac{1}{2} \int_0^1 \tilde{\mathbf{B}} \left(\boldsymbol{\Psi}(\mathbf{Q}^-, \mathbf{Q}^+, s) \right) \cdot \tilde{\mathbf{n}} \, \frac{\partial \boldsymbol{\Psi}}{\partial s} \, ds.$$

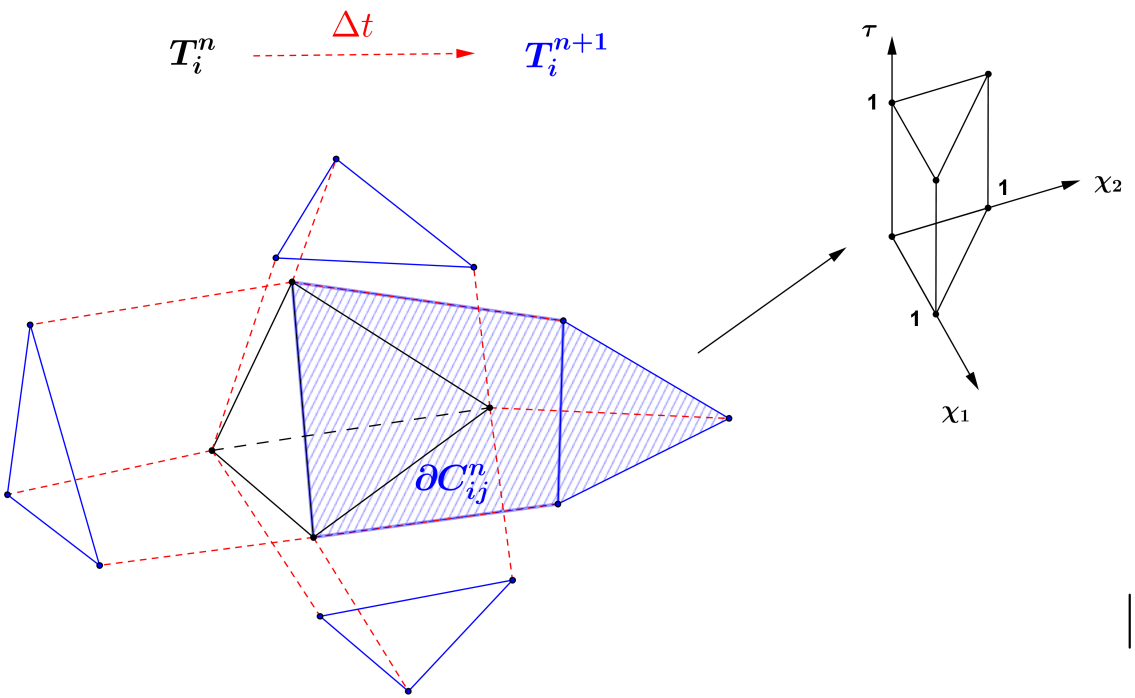

Linear parametrization

$$\partial C_{ij}^n = \tilde{\mathbf{x}}(\chi_1, \chi_2, \tau)$$

$$= \sum_{k=1}^{6} \beta_k(\chi_1, \chi_2, \tau) \tilde{\mathbf{X}}_{ij,k}^n$$

$$0 \le \tilde{\chi} = (\chi_1, \chi_2, \tau) \le 1$$

$$|\partial C_{ij}^n| = \left| \frac{\partial \tilde{\mathbf{x}}}{\partial \tilde{\chi}} \right|, \quad \tilde{\mathbf{n}}_{ij} = \frac{\partial \tilde{\mathbf{x}}}{\partial \tilde{\chi}} / |\partial C_{ij}^n|$$

Finite Volume Scheme

ALE–type One–Step Finite Volume Scheme

$$|T_i^{n+1}|\,\mathbf{Q}_i^{n+1} = |T_i^n|\,\mathbf{Q}_i^n - \sum_{T_j \in \mathcal{N}_i} \int_0^1 \int_0^1 |\partial C_{ij}^n| \tilde{\mathbf{G}}_{ij}\, d\chi d\tau + \int_{\mathcal{C}_i^n \setminus \partial \mathcal{C}_i^n} (\mathbf{S}_h - \mathbf{P}_h)\, d\mathbf{x}dt$$

Finite Volume Scheme

ALE–type One–Step Finite Volume Scheme

$$|T_i^{n+1}|\,\mathbf{Q}_i^{n+1} = |T_i^n|\,\mathbf{Q}_i^n - \sum_{T_j \in \mathcal{N}_i} \int_0^1 \int_0^1 |\partial C_{ij}^n| \tilde{\mathbf{G}}_{ij}\, d\chi d\tau + \int_{\mathcal{C}_i^n \setminus \partial \mathcal{C}_i^n} (\mathbf{S}_h - \mathbf{P}_h)\, d\mathbf{x}dt$$

Rusanov numerical flux

$$\tilde{\mathbf{G}}_{ij} = \frac{1}{2}\left(\tilde{\mathbf{F}}(\mathbf{q}_h^+) + \tilde{\mathbf{F}}(\mathbf{q}_h^-)\right) \cdot \tilde{\mathbf{n}}_{ij} + \frac{1}{2}\left(\int_0^1 \tilde{\mathbf{B}}(\boldsymbol{\Psi}) \cdot \tilde{\mathbf{n}}\, ds - |\lambda_{\max}|\mathbf{I}\right)(\mathbf{q}_h^+ - \mathbf{q}_h^-)$$

$$\tilde{\mathbf{A}}_{\tilde{\mathbf{n}}} = \tilde{\mathbf{A}} \cdot \tilde{\mathbf{n}} = \left(\sqrt{\tilde{n}_x^2 + \tilde{n}_y^2 + \tilde{n}_z^2}\right)\left[\left(\frac{\partial \mathbf{F}}{\partial \mathbf{Q}} + \mathbf{B}\right) \cdot \mathbf{n} - (\mathbf{V} \cdot \mathbf{n})\,\mathbf{I}\right], \quad \mathbf{n} = \frac{(\tilde{n}_x, \tilde{n}_y, \tilde{n}_z)^T}{\sqrt{\tilde{n}_x^2 + \tilde{n}_y^2 + \tilde{n}_z^2}}$$

Finite Volume Scheme

ALE–type One–Step Finite Volume Scheme

$$|T_i^{n+1}|\,\mathbf{Q}_i^{n+1} = |T_i^n|\,\mathbf{Q}_i^n - \sum_{T_j \in \mathcal{N}_i} \int_0^1 \int_0^1 |\partial C_{ij}^n| \tilde{\mathbf{G}}_{ij}\, d\chi d\tau + \int_{\mathcal{C}_i^n \setminus \partial \mathcal{C}_i^n} (\mathbf{S}_h - \mathbf{P}_h)\, d\mathbf{x}dt$$

Osher numerical flux

$$\tilde{\mathbf{G}}_{ij} = \frac{1}{2}\left(\tilde{\mathbf{F}}(\mathbf{q}_h^+) + \tilde{\mathbf{F}}(\mathbf{q}_h^-)\right)\cdot \tilde{\mathbf{n}}_{ij} + \frac{1}{2}\left(\int_0^1 \left(\tilde{\mathbf{B}}(\boldsymbol{\Psi})\cdot\tilde{\mathbf{n}} - \left|\tilde{\mathbf{A}}_{\tilde{\mathbf{n}}}(\boldsymbol{\Psi})\right|\right) ds\right)(\mathbf{q}_h^+ - \mathbf{q}_h^-)$$

$$\boldsymbol{\Psi} = \boldsymbol{\Psi}(\mathbf{Q}^-, \mathbf{Q}^+, s) = \mathbf{Q}^- + s(\mathbf{Q}^+ - \mathbf{Q}^-), \qquad 0 \le s \le 1$$

$$|\mathbf{A}| = \mathbf{R}|\boldsymbol{\Lambda}|\mathbf{R}^{-1}, \qquad |\boldsymbol{\Lambda}| = \mathrm{diag}\left(|\lambda_1|, |\lambda_2|, ..., |\lambda_\nu|\right)$$

Outline

1. Introduction
2. Numerical Method
   - Hyperbolic Balance Laws
   - High Order WENO Reconstruction on Unstructured Meshes
   - Local Space-Time DG Predictor on Moving Meshes
   - Mesh Motion
   - Solution Algorithm
3. Validation
   - The Euler equations
   - The Baer–Nunziato Model
4. Conclusions and Outlook

The Euler equations

$$\mathbf{Q}_t + \mathbf{f}_x + \mathbf{g}_y + \mathbf{h}_z = \mathbf{S}(\mathbf{Q})$$

with

$$\mathbf{Q} = \begin{pmatrix} \rho \\ \rho v_j \\ \rho E \end{pmatrix}, \quad \mathbf{F} = (\mathbf{f}, \mathbf{g}, \mathbf{h}) = \begin{pmatrix} \rho v_i \\ \rho v_i v_j + p\delta_{ij} \\ v_i(\rho E + p) \end{pmatrix}.$$

$\rho \rightarrow$ fluid density

$\mathbf{v} = (v_x, v_y, v_z) \rightarrow$ fluid's velocity vector

$\mathbf{S} \rightarrow$ vector of source term ($\mathbf{S} = 0$)

$p \rightarrow$ fluid pressure

$$p = (\gamma - 1)\left(\rho E - \frac{1}{2}\rho(v_x^2 + v_y^2 + v_z^2)\right)$$

$\downarrow$

equation of state

Convergence studies: *Shu* Vortex

(Hu and Shu, *JCP* 150: 97-127 , 1999)

$$\text{IC: } (\rho, v_x, v_y, v_z, p) = (1 + \delta\rho, 1 + \delta v_x, 1 + \delta v_y, 0, 1 + \delta p)$$

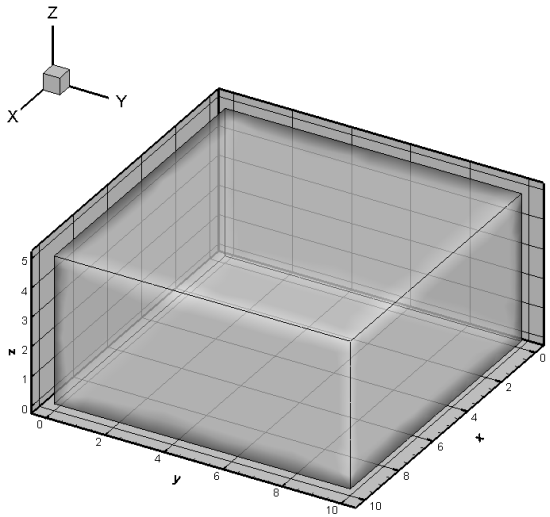

Computational domain

$$\Omega(0) = [0; 10] \times [0; 10] \times [0; 5]$$

Convective velocity

$$\mathbf{v}_c = (1, 1, 0)$$

Perturbations

$$\begin{bmatrix} \delta v_x \\ \delta v_y \\ \delta v_z \end{bmatrix} = \frac{\epsilon}{2\pi} e^{\frac{1-r^2}{2}} \begin{bmatrix} -(y-5) \\ (x-5) \\ 0 \end{bmatrix}$$

$$\delta S = 0$$

$$\delta T = \frac{(\gamma-1)\epsilon^2}{8\gamma\pi^2} e^{1-r^2}$$

Parameters

$$r^2 = (x-5)^2 + (y-5)^2 \text{ radius}$$

$$\epsilon = 5 \text{ vortex strength}$$

$$\gamma = 1.4 \text{ ratio of specific heat}$$

Convergence studies: *Shu* Vortex

(Hu and Shu, *JCP* 150: 97-127 , 1999)

$h(\Omega(t_f))$	ϵ_{L_2}	$\mathcal{O}(L_2)$	$h(\Omega, t_f)$	ϵ_{L_2}	$\mathcal{O}(L_2)$
	$\mathcal{O}1$			$\mathcal{O}2$	
3.43E-01	1.081E-01	-	2.89E-01	2.214E-02	-
2.85E-01	9.159E-02	0.9	2.16E-01	1.202E-02	2.1
2.09E-01	6.875E-02	0.9	1.52E-01	5.865E-03	2.0
1.47E-01	4.899E-02	1.0	1.13E-01	3.254E-03	2.0
	$\mathcal{O}3$			$\mathcal{O}4$	
2.89E-01	1.718E-02	-	2.89E-01	4.116E-03	-
2.17E-01	7.641E-03	2.8	2.17E-01	1.369E-03	3.8
1.52E-01	2.601E-03	3.1	1.52E-01	3.273E-04	4.1
1.13E-01	1.049E-03	3.1	1.13E-01	9.802E-05	4.1
	$\mathcal{O}5$			$\mathcal{O}6$	
2.89E-01	2.272E-03	-	2.89E-01	1.015E-03	-
2.17E-01	6.605E-04	4.3	2.17E-01	2.312E-04	5.1
1.52E-01	1.234E-04	4.8	1.52E-01	3.090E-05	5.7
1.13E-01	2.932E-05	4.9	1.13E-01	6.576E-06	5.2

Three–dimensional Explosion Problem

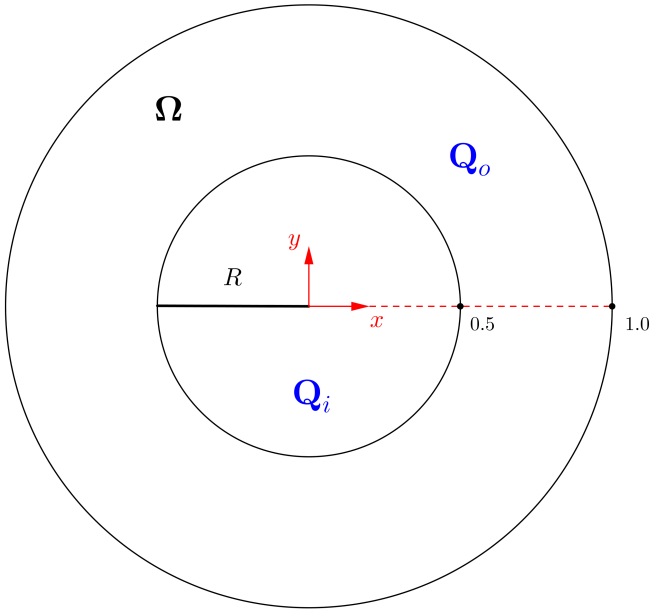

	ρ	v_x	v_y	v_z	p
Inner state ($\mathbf{Q}_i$)	1.0	0.0	0.0	0.0	1.0
Outer state ($\mathbf{Q}_o$)	0.125	0.0	0.0	0.0	0.1

Parameters

$$r^2 = x^2 + y^2 + z^2 \text{ radius}$$
$$R = 0.5 \text{ internal radius}$$
$$\gamma = 1.4 \text{ ratio of specific heat}$$

Analytical solution

$$\mathbf{Q}_t + \mathbf{F}(\mathbf{Q})_r = \mathbf{S}(\mathbf{Q})$$

$$\mathbf{Q} = \begin{pmatrix} \rho \\ \rho u \\ \rho E \end{pmatrix}, \quad \mathbf{F} = \begin{pmatrix} \rho u \\ \rho u^2 + p \\ u(\rho E + p) \end{pmatrix}, \quad \mathbf{S} = -\frac{\alpha}{r} \begin{pmatrix} \rho u \\ \rho u^2 \\ u(\rho E + p) \end{pmatrix} \qquad \alpha = 2$$

Three–dimensional Explosion Problem

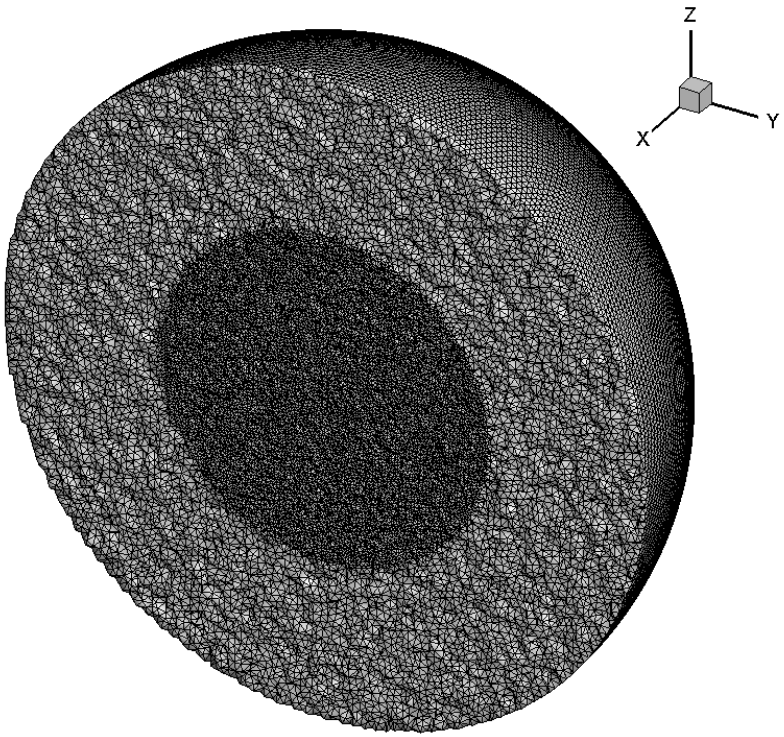

$t = 0.00$

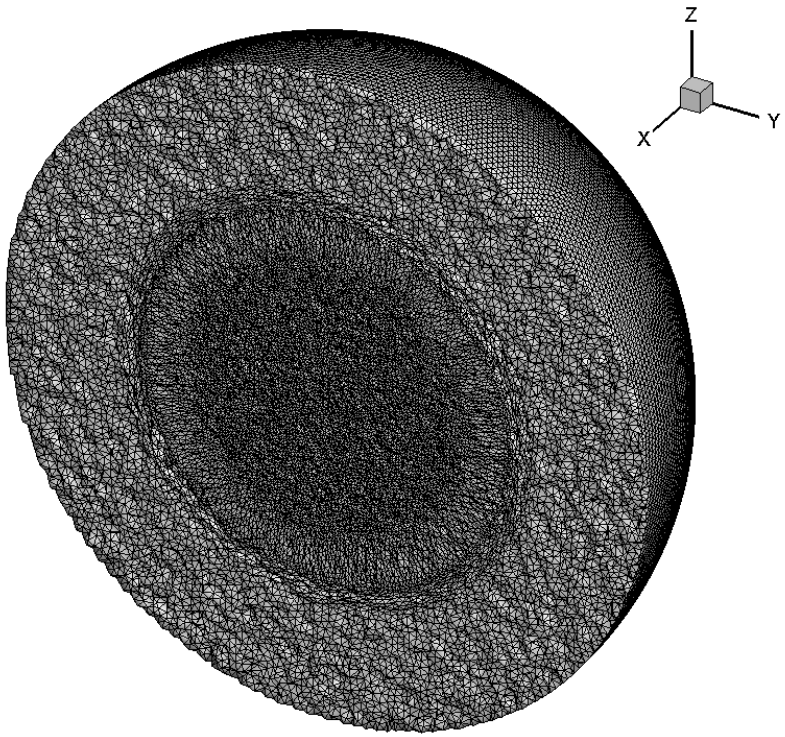

$t = 0.08$

4^{th} order accurate explosion problem with $N_E = 7225720$.

Three–dimensional Explosion Problem

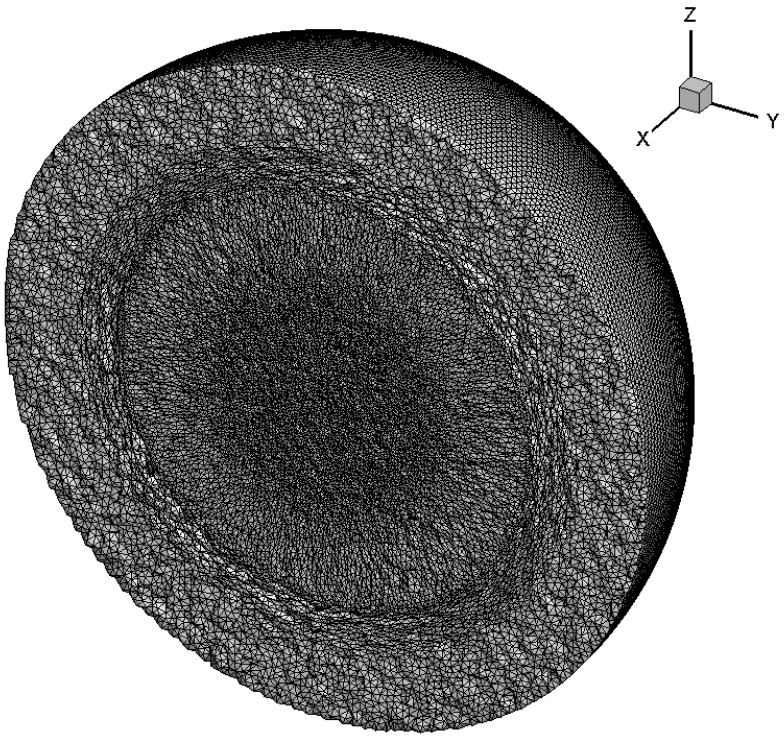

$t = 0.16$

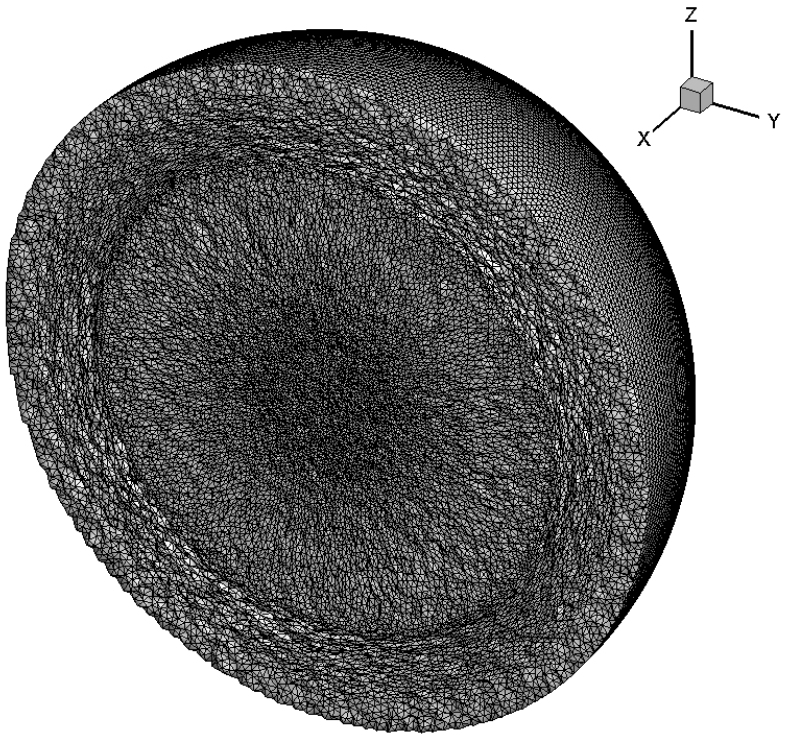

$t = 0.25$

4^{th} order accurate explosion problem with $N_E = 7225720$.

Three–dimensional Explosion Problem

Density profile

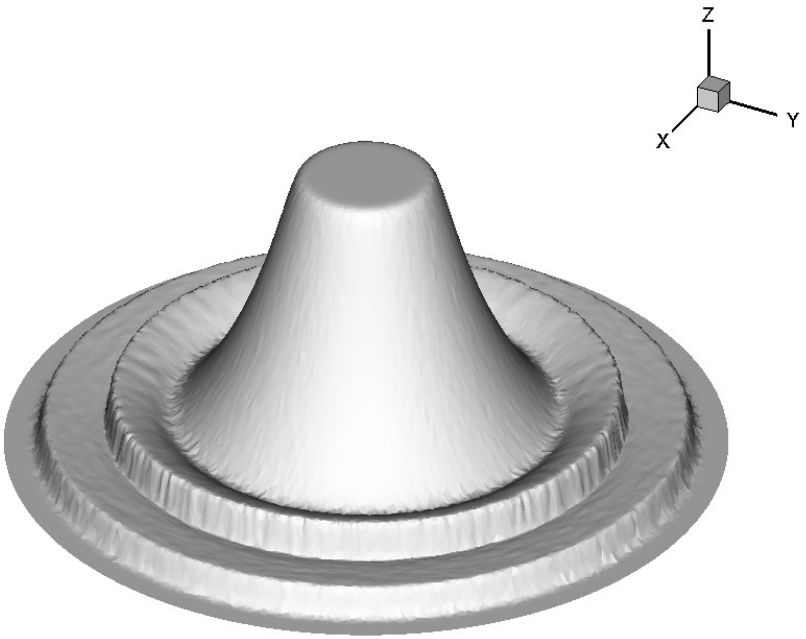

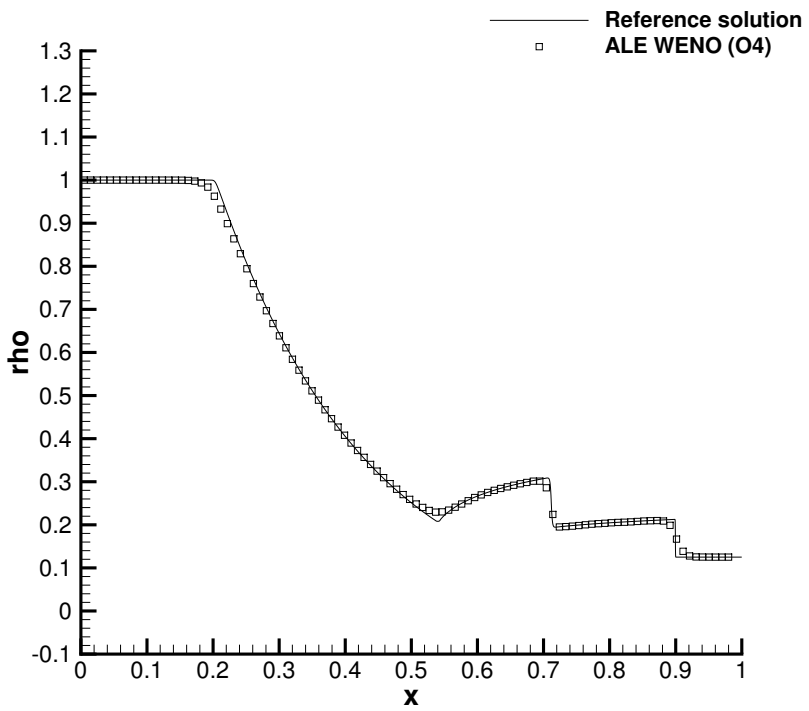

4^{th} order accurate explosion problem with $N_E = 7225720$.

Three–dimensional Explosion Problem

Velocity and pressure profile

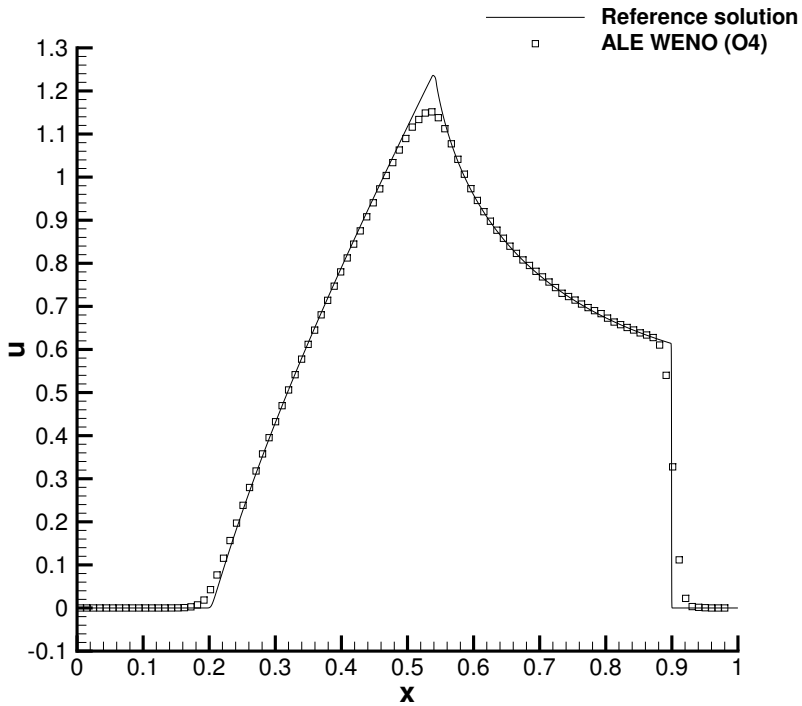

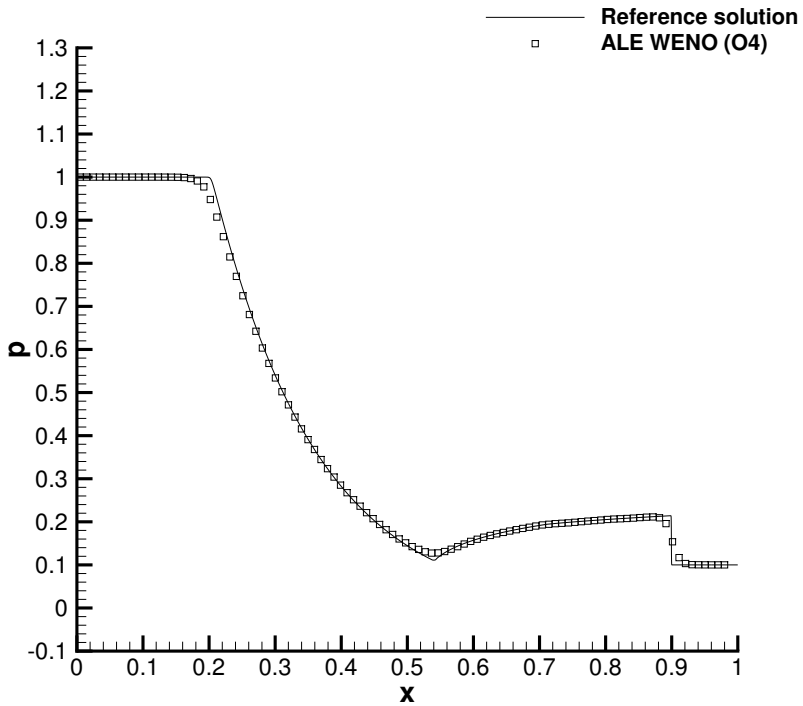

4^{th} order accurate explosion problem with $N_E = 7225720$.

The Kidder problem (Kidder, *Nucl. Fusion* 1: 3-14 , 1976)

IC:

$$\rho_0 = \rho(r,0) = \left(\frac{r_{e,0}^2 - r^2}{r_{e,0}^2 - r_{i,0}^2} \rho_{i,0}^{\gamma-1} + \frac{r^2 - r_{i,0}^2}{r_{e,0}^2 - r_{e,0}^2} \rho_{e,0}^{\gamma-1} \right)^{\frac{1}{\gamma-1}}$$

$$s_0 = \frac{p_0}{\rho_0^\gamma} = 1$$

$$p_0(r) = s_0 \rho_0(r)^\gamma$$

Parameters

$r_e(0) = 1.0$ external radius

$r_i(0) = 0.9$ internal radius

$\gamma = 5/3$ ratio of specific heat

$\rho_{i,0} = 1.0$ initial internal density

$\rho_{e,0} = 2.0$ initial external density

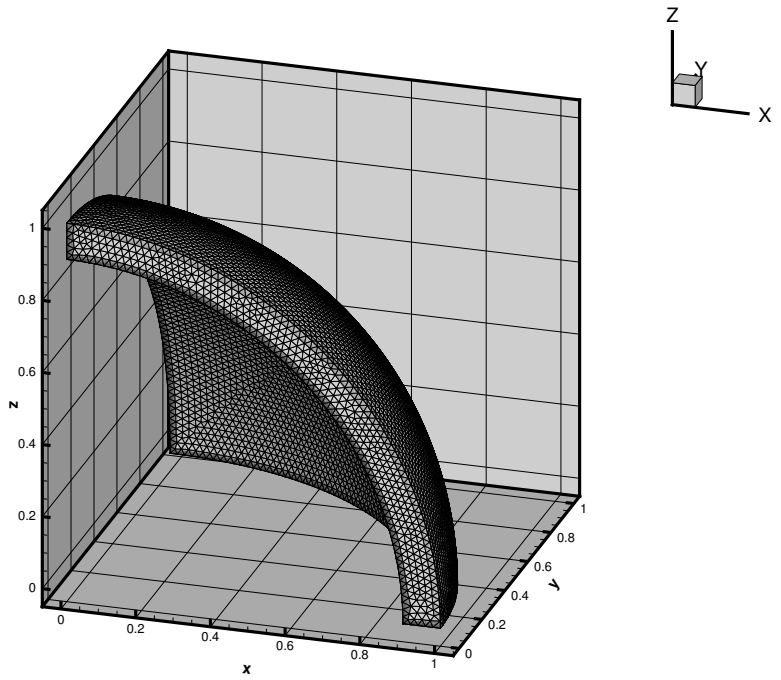

The Kidder problem (Kidder, *Nucl. Fusion* 1: 3-14 , 1976)

Analytical Solution

$$\begin{aligned}
\rho\left(R(r,t),t\right) &= h(t)^{-\frac{2}{\gamma-1}}\rho_0\left[\frac{R(r,t)}{h(t)}\right] \\
u_r\left(R(r,t),t\right) &= \frac{d}{dt}h(t)\left[\frac{R(r,t)}{h(t)}\right] \\
p\left(R(r,t),t\right) &= h(t)-\frac{2\gamma}{\gamma-1}p_0\left[\frac{R(r,t)}{h(t)}\right]
\end{aligned}$$

with

$$h(t)=\sqrt{1-\frac{t^2}{\tau^2}}, \quad \tau=\sqrt{\frac{\gamma-1}{2}\frac{(r_{e,0}^2-r_{i,0}^2)}{c_{e,0}^2-c_{i,0}^2}}$$

and the internal and external sound speeds c_i and c_e defined as

$$c_i=\sqrt{\gamma\frac{p_i}{\rho_i}}, \qquad c_e=\sqrt{\gamma\frac{p_e}{\rho_e}}$$

The Kidder problem (Kidder, *Nucl. Fusion* 1: 3-14 , 1976)

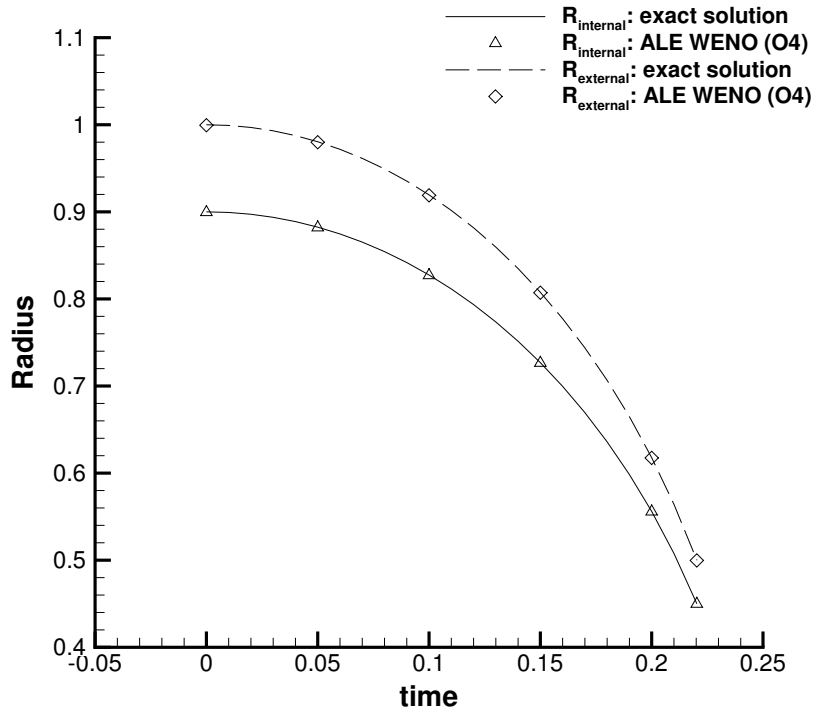

	r_{ex}	r_{num}	$\|err\|$
Internal radius	0.450000	0.449765	2.35E-04
External radius	0.500000	0.499728	2.72E-04

The Saltzman problem (Dukovicz et al., *JCP* 99: 115-134 , 1992)

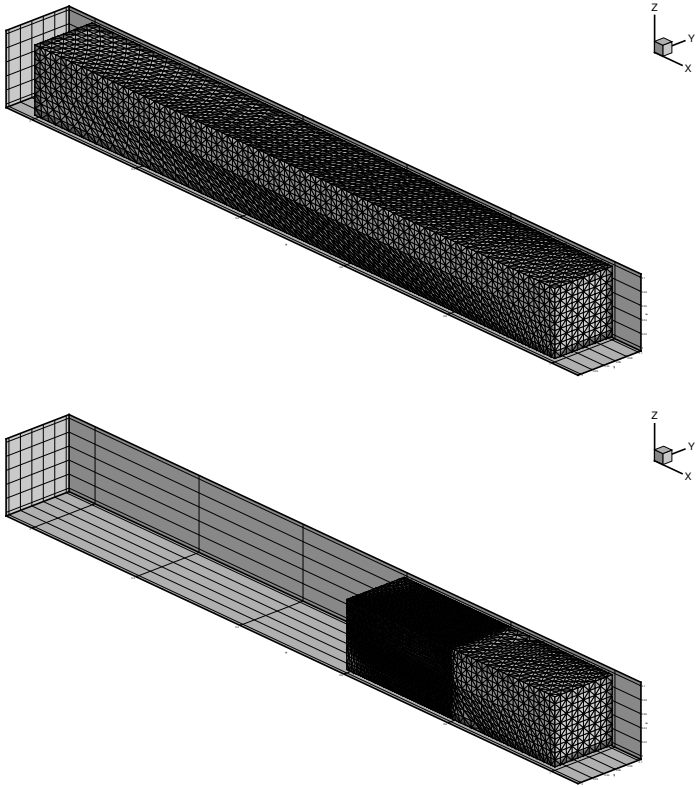

Computational domain
$\Omega(0) = [0;1] \times [0;0.1] \times [0;0.1]$

Piston velocity
$\mathbf{v}_p = (1,0,0)$

Mesh size
$100 \times 10 \times 10$ cubes

IC:
$\rho_0 = 1$, $\mathbf{v}_0 = \mathbf{0}$, $e_0 = 10^{-4}$

Analytical solution

	Left state	*Right state*
ρ	1.0	1.0
u	1.0	-1.0
p	$6.67 \cdot 10^{-5}$	$6.67 \cdot 10^{-5}$

final time:	$t_f = 0.6$
shifting:	$d = u_p \cdot t_f$
final shock location:	$x = 0.8$
exact density:	$\rho_e = 4.0$

The Saltzman problem (Dukovicz et al., *JCP* 99: 115-134 , 1992)

The Saltzman problem (Dukovicz et al., *JCP* 99: 115-134 , 1992)

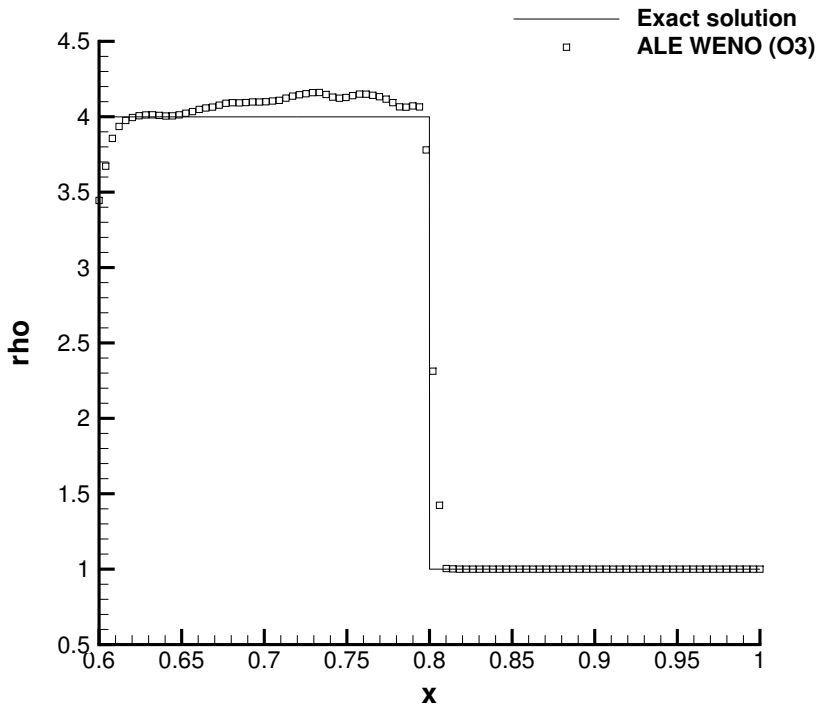

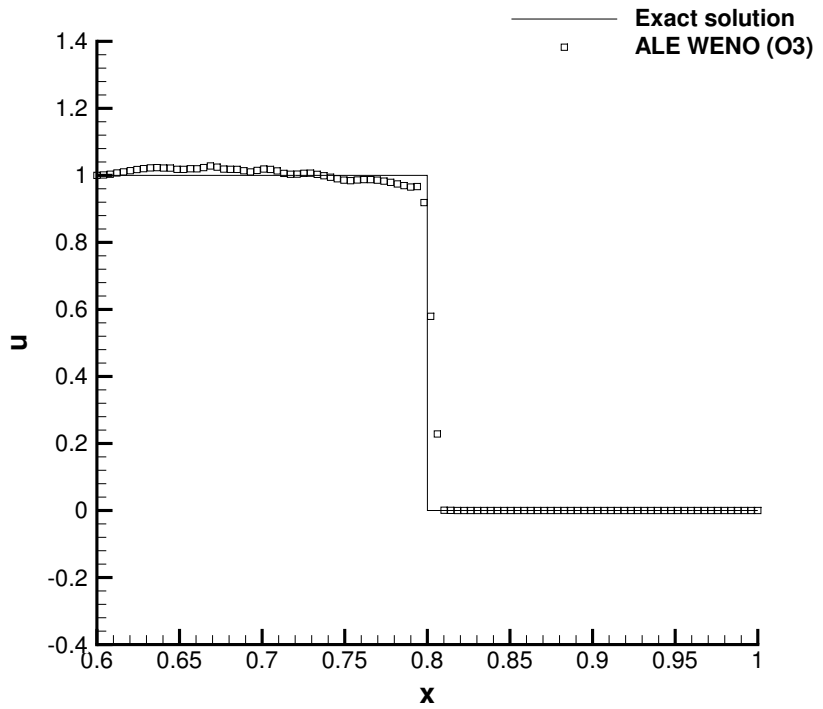

3^{rd} order numerical results of density and velocity for the Saltzman problem.

The Sedov Problem

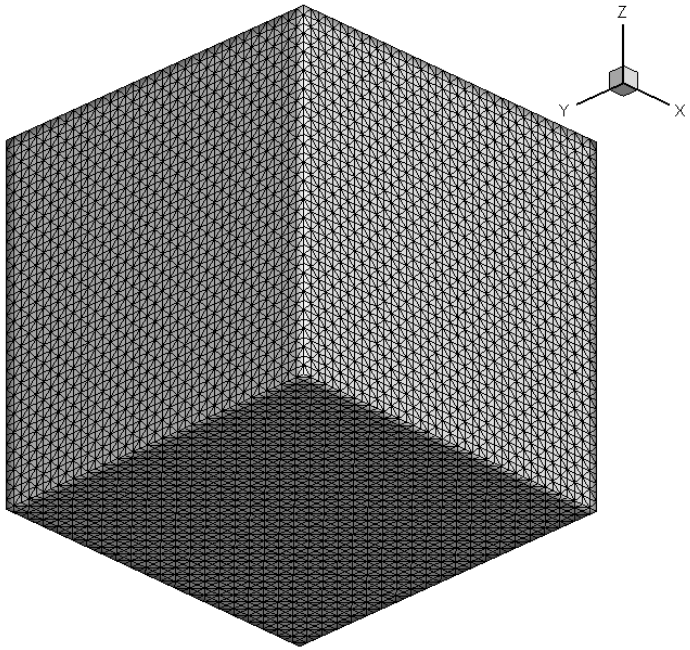

Computational domain
$\Omega(0) = [0; 1.2] \times [0; 1.2] \times [0; 1.2]$

Mesh size
$40 \times 40 \times 40$ cubes

IC:
$\rho_0 = 1$, $\mathbf{v}_0 = \mathbf{0}$, $\gamma = 1.4$, $E_{tot} = 0.851072$

$$p_0 = \begin{cases} (\gamma - 1)\rho_0 \frac{E_{tot}}{8 \cdot V_{or}} & \text{in } c_{or}, \\ 10^{-6} & \text{elsewhere.} \end{cases}$$

Analytical solution $\Rightarrow$ Kamm et al., *Technical Report LA-UR-07-2849, LANL*, 2007

The Sedov Problem

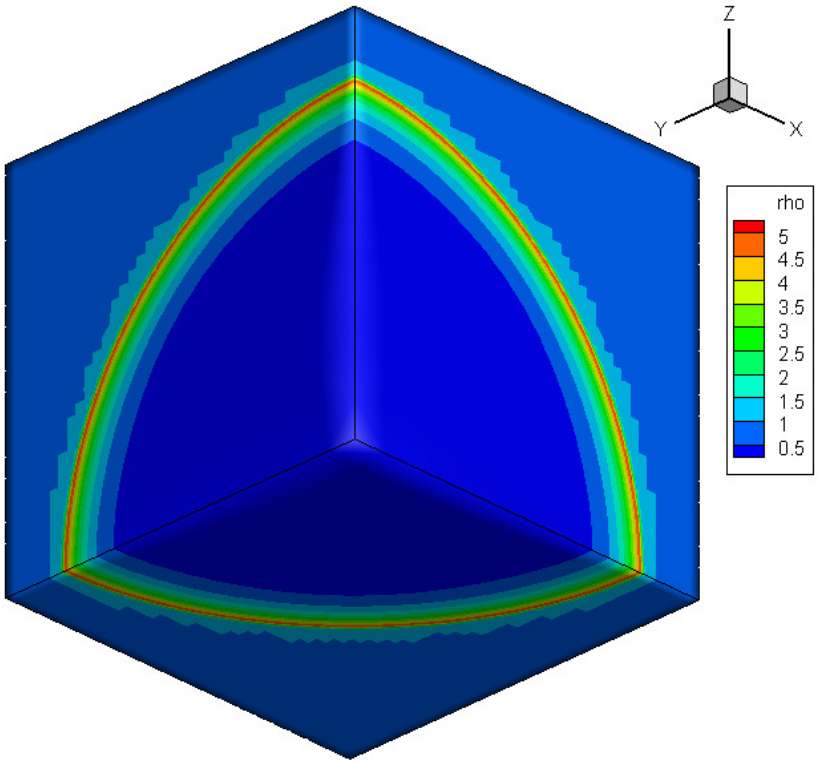

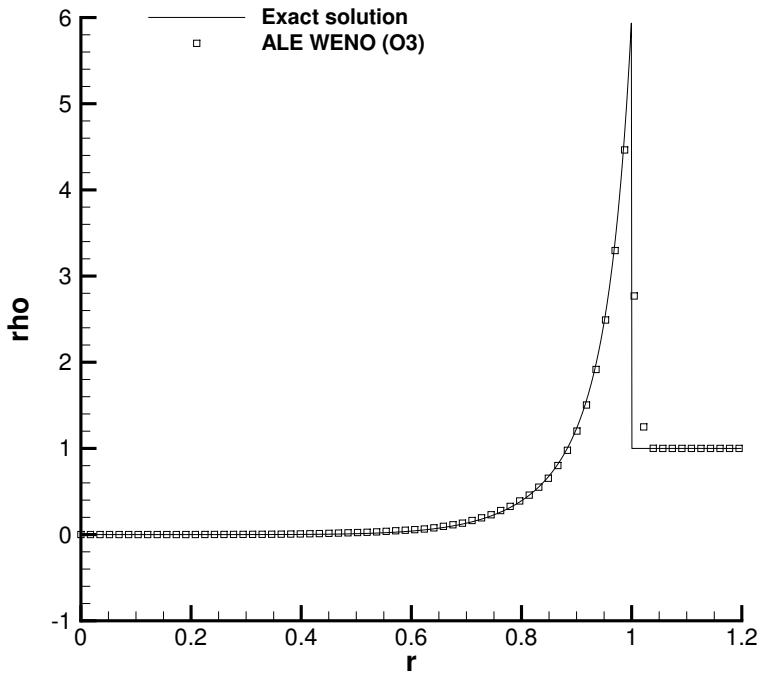

3^{rd} order accurate numerical results for the Sedov problem.

The Sedov Problem

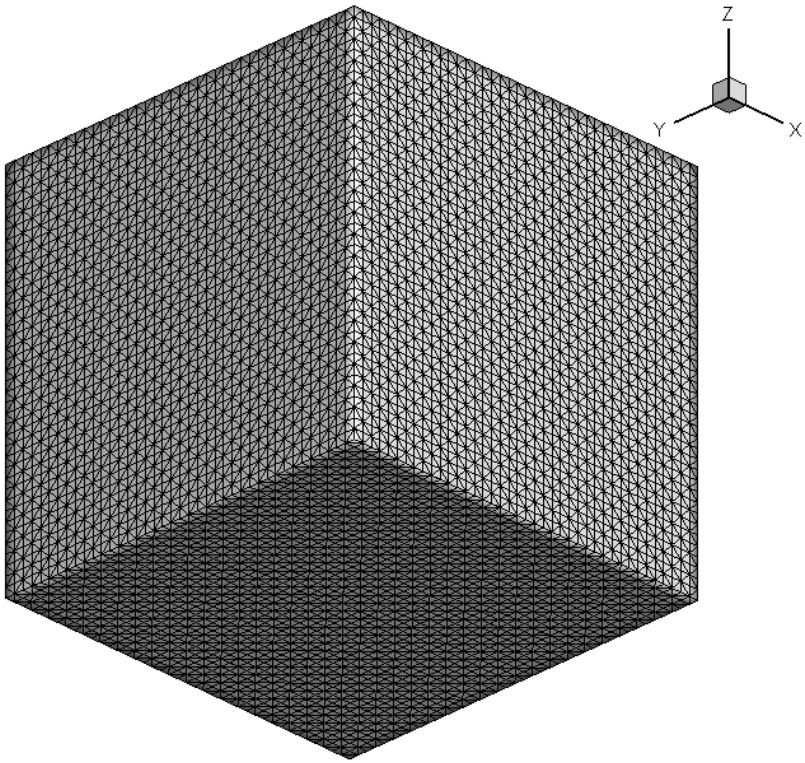

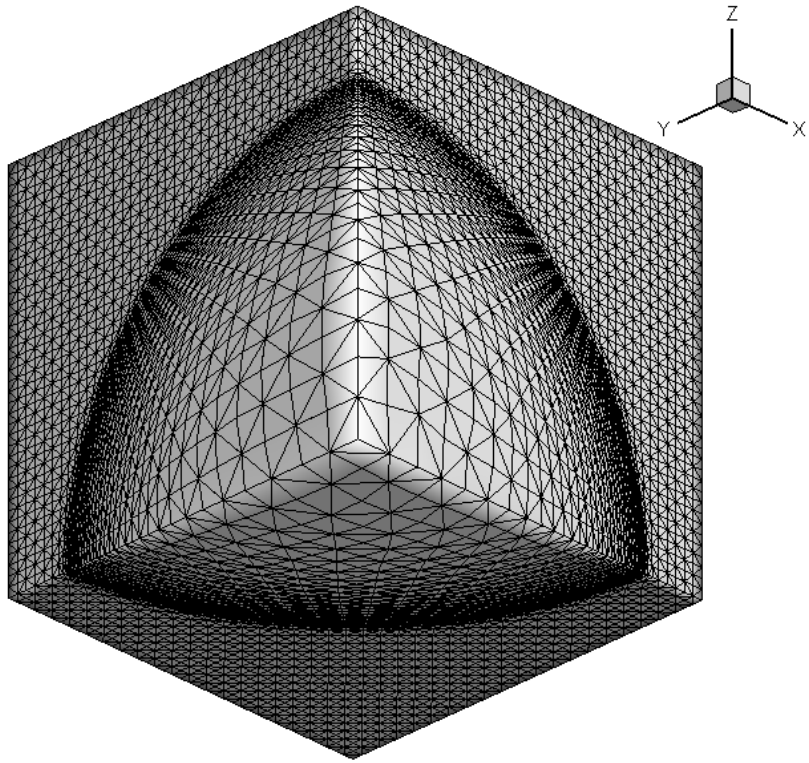

3^{rd} order accurate numerical results for the Sedov problem.

Outline

1. Introduction
2. Numerical Method
   - Hyperbolic Balance Laws
   - High Order WENO Reconstruction on Unstructured Meshes
   - Local Space-Time DG Predictor on Moving Meshes
   - Mesh Motion
   - Solution Algorithm
3. Validation
   - The Euler equations
   - The Baer–Nunziato Model
4. Conclusions and Outlook

The Baer-Nunziato Model of Compressible Multi-Phase Flows

$$
\left.
\begin{aligned}
&\frac{\partial}{\partial t}\left(\phi_1\rho_1\right) + \nabla\cdot\left(\phi_1\rho_1\mathbf{u_1}\right) = 0,\\
&\frac{\partial}{\partial t}\left(\phi_1\rho_1\mathbf{u_1}\right) + \nabla\cdot\left(\phi_1\rho_1\mathbf{u_1}\mathbf{u_1}\right) + \nabla\phi_1 p_1 = p_I\nabla\phi_1 - \lambda\left(\mathbf{u_1}-\mathbf{u_2}\right),\\
&\frac{\partial}{\partial t}\left(\phi_1\rho_1 E_1\right) + \nabla\cdot\left(\left(\phi_1\rho_1 E_1 + \phi_1 p_1\right)\mathbf{u_1}\right) = -p_I\partial_t\phi_1 - \lambda\,\mathbf{u_I}\cdot\left(\mathbf{u_1}-\mathbf{u_2}\right),\\
&\frac{\partial}{\partial t}\left(\phi_2\rho_2\right) + \nabla\cdot\left(\phi_2\rho_2\mathbf{u_2}\right) = 0,\\
&\frac{\partial}{\partial t}\left(\phi_2\rho_2\mathbf{u_2}\right) + \nabla\cdot\left(\phi_2\rho_2\mathbf{u_2}\mathbf{u_2}\right) + \nabla\phi_2 p_2 = p_I\nabla\phi_2 - \lambda\left(\mathbf{u_2}-\mathbf{u_1}\right),\\
&\frac{\partial}{\partial t}\left(\phi_2\rho_2 E_2\right) + \nabla\cdot\left(\left(\phi_2\rho_2 E_2 + \phi_2 p_2\right)\mathbf{u_2}\right) = p_I\partial_t\phi_1 - \lambda\,\mathbf{u_I}\cdot\left(\mathbf{u_2}-\mathbf{u_1}\right),\\
&\frac{\partial}{\partial t}\phi_1 + \mathbf{u_I}\nabla\phi_1 = \nu(p_1 - p_2).
\end{aligned}
\right\}
$$

The Baer-Nunziato Model of Compressible Multi-Phase Flows

Definitions

k	$\rightarrow$	phase
ϕ_k	$\rightarrow$	volume fraction of phase k
$\mathbf{u_k}$	$\rightarrow$	velocity vector of phase k
subscripts 1	$\rightarrow$	solid phase
subscripts 2	$\rightarrow$	gas phase
subscripts I	$\rightarrow$	interface
e_k	$\rightarrow$	internal energy
$E_k = e_k + \frac{1}{2}\mathbf{u_k}^2$	$\rightarrow$	specific total energy of phase k

Assumptions

$\phi_1 + \phi_2 = 1$	volume fractions must sum to the unity
$\mathbf{u_I} = \mathbf{u_1}$	interface velocity is the solid phase velocity
$p_I = p_2$	interface pressure is the gas phase pressure [a]

[a] according to the original formulation of the model (M.R. Baer and J.W. Nunziato, *J. of Multiphase Flows* 1986)

Riemann problems

Initial condition for the left state (L) and the right state (R) for the Riemann problems solved with the Baer-Nunziato model. Values for γ_k, π_k and the final time t_f are also given.

	ρ_s	u_s	p_s	ρ_g	u_g	p_g	ϕ_s	t_f
RP1:	$\gamma_s = 1.4$,	$\pi_s = 0$,	$\gamma_g = 1.4$,	$\pi_g = 0$,	$\lambda = \mu = 0$			
L	1.0	0.0	1.0	0.5	0.0	1.0	0.4	0.10
R	2.0	0.0	2.0	1.5	0.0	2.0	0.8	
RP2 :	$\gamma_s = 3.0$,	$\pi_s = 100$,	$\gamma_g = 1.4$,	$\pi_g = 0$,	$\lambda = \mu = 0$			
L	800.0	0.0	500.0	1.5	0.0	2.0	0.4	0.10
R	1000.0	0.0	600.0	1.0	0.0	1.0	0.3	
RP3 :	$\gamma_s = 1.4$,	$\pi_s = 0$,	$\gamma_g = 1.67$,	$\pi_g = 0$,	$\lambda = 10^3$,	$\mu = 10^2$		
L	1.0	0.0	1.0	1.0	0.0	1.0	0.99	0.2
R	0.125	0.0	0.1	0.125	0.0	0.1	0.01	
RP4 :	$\gamma_s = 2.0$,	$\pi_s = 0$,	$\gamma_g = 1.4$,	$\pi_g = 0$,	$\lambda = 10^3$,	$\mu = 10^2$		
L	1.0	0.0	2.0	1.0	0.0	2.0	0.99	0.2
R	0.125	0.0	0.1	0.125	0.0	0.1	0.01	

Riemann problems

RP1

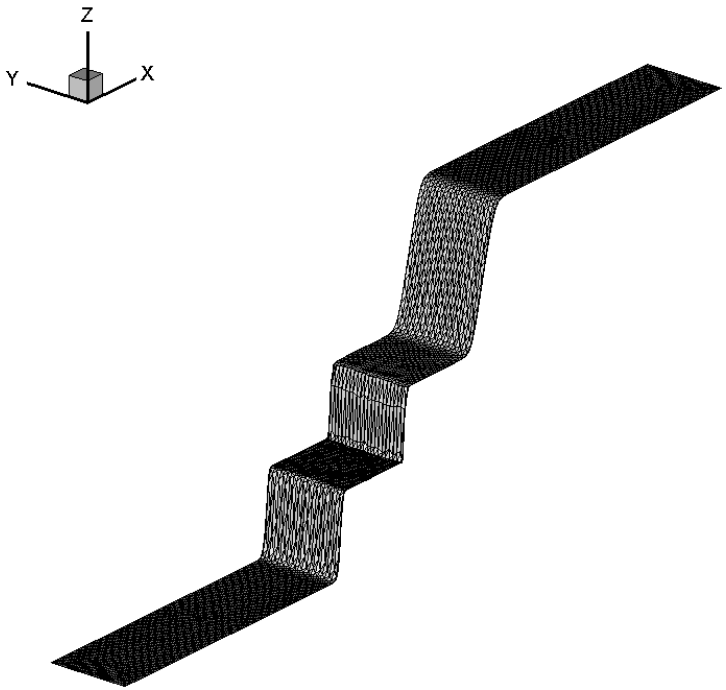

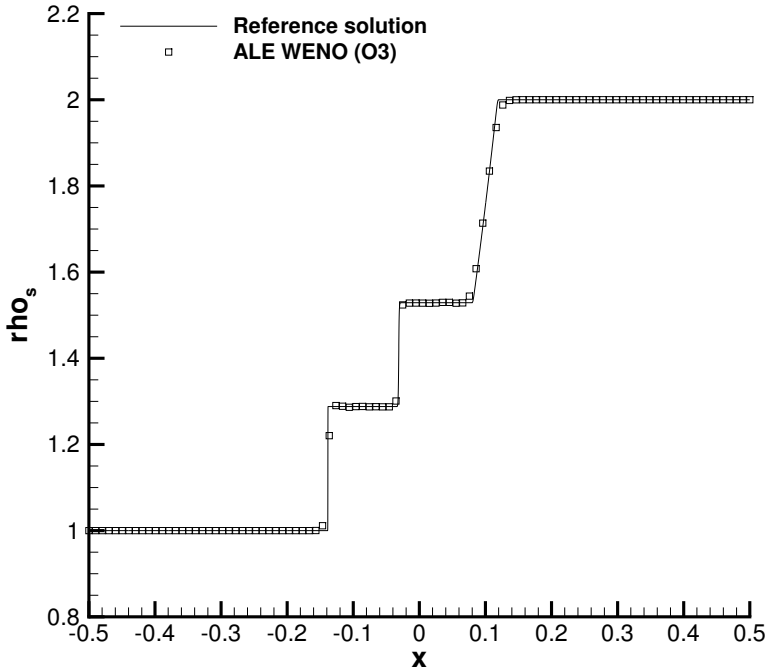

3^{rd} order accurate density distribution for the Riemann problem RP1.

Riemann problems

RP2

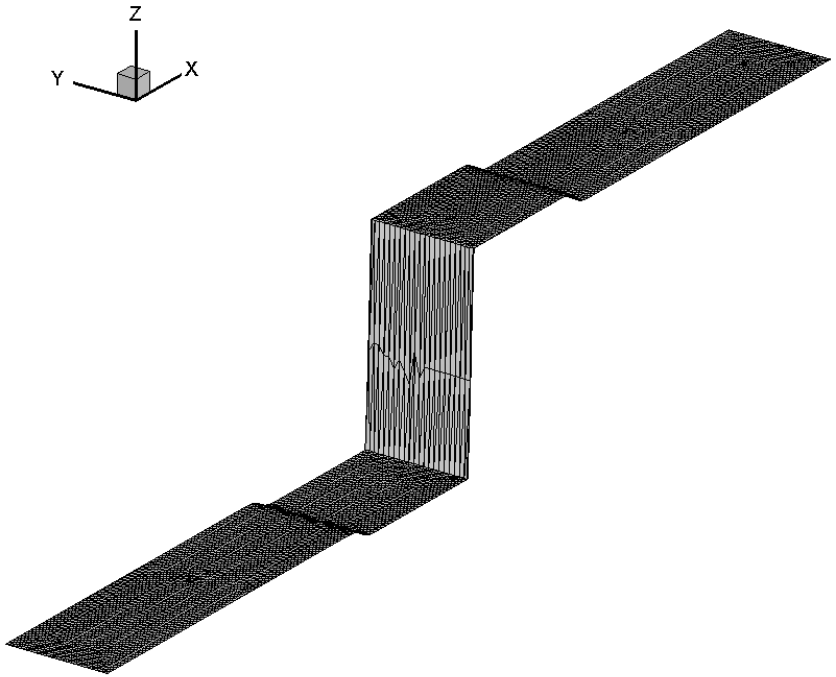

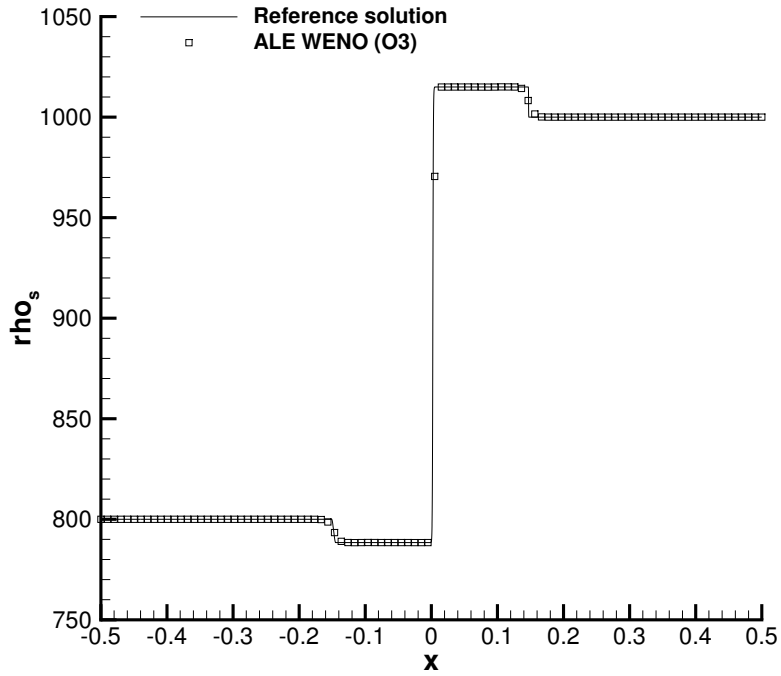

3^{rd} order accurate density distribution for the Riemann problem RP2.

Riemann problems

RP3

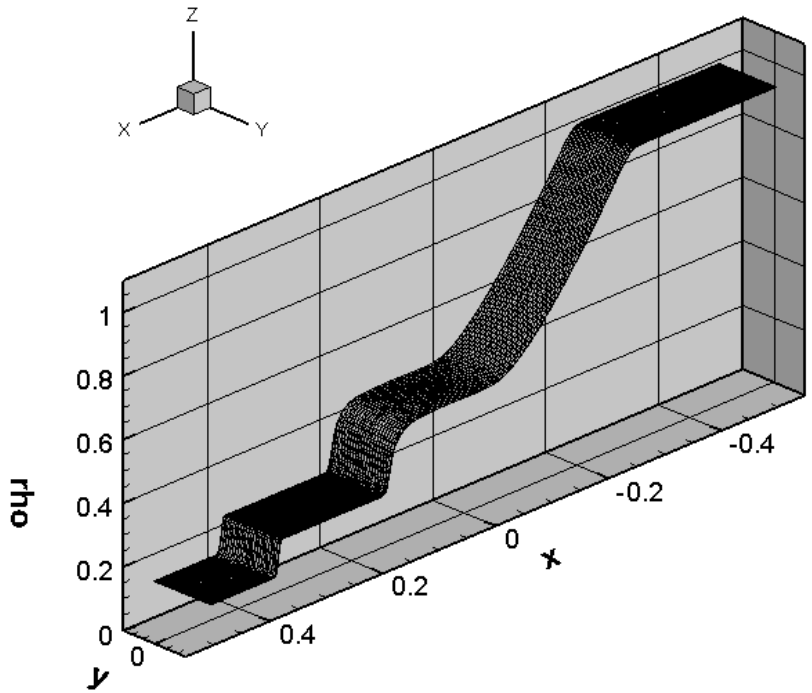

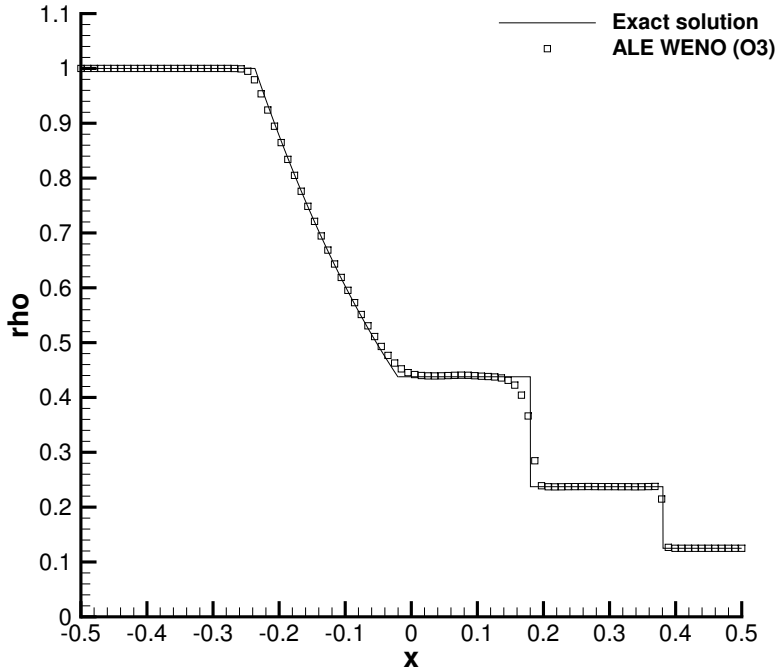

3^{rd} order accurate density distribution for the Riemann problem RP3.

Riemann problems

RP4

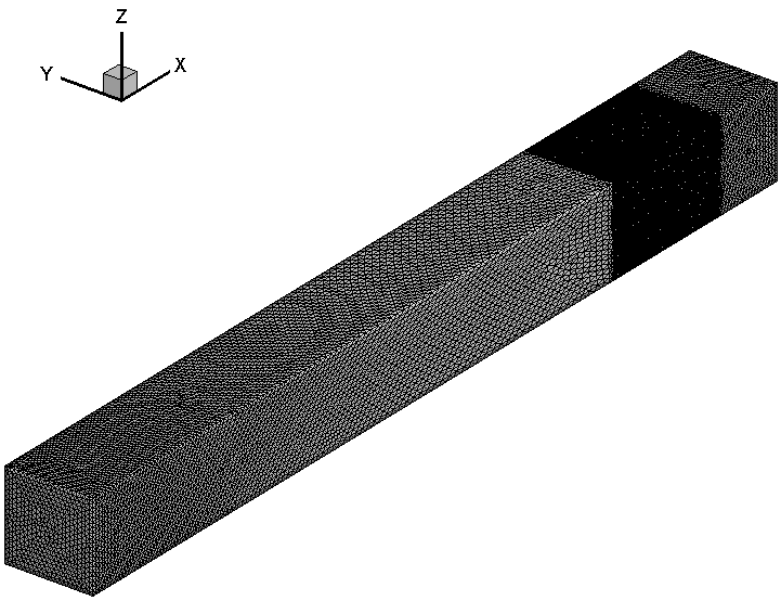

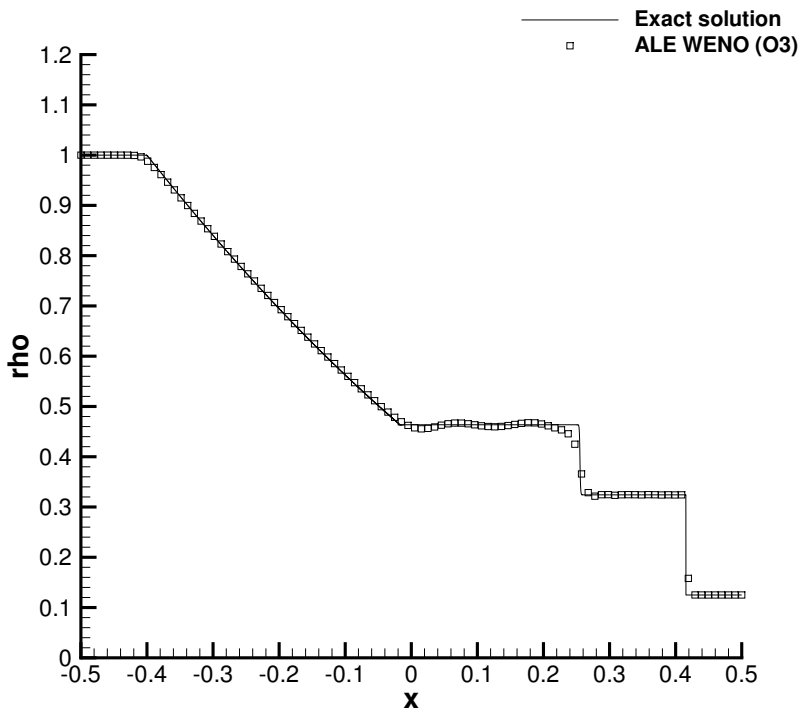

3^{rd} order accurate density distribution for the Riemann problem RP4.

Explosion problems

EP1

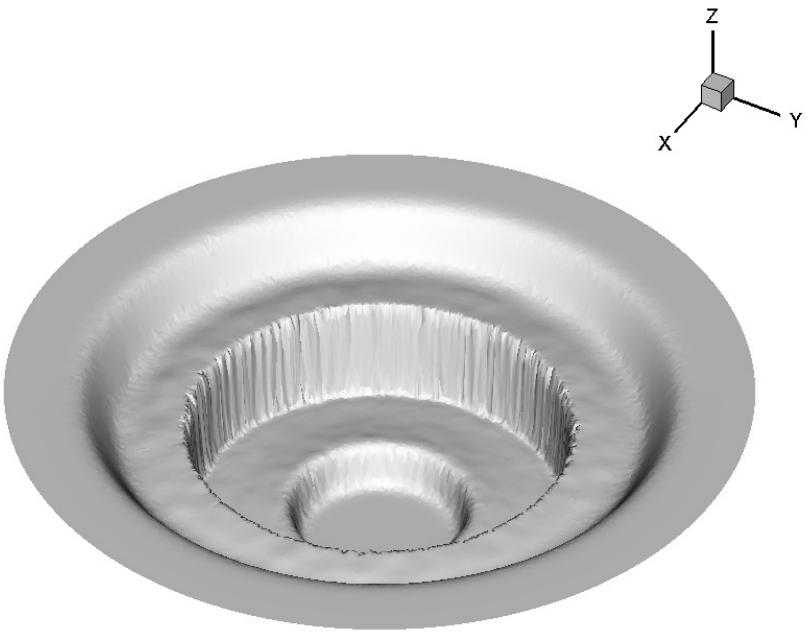

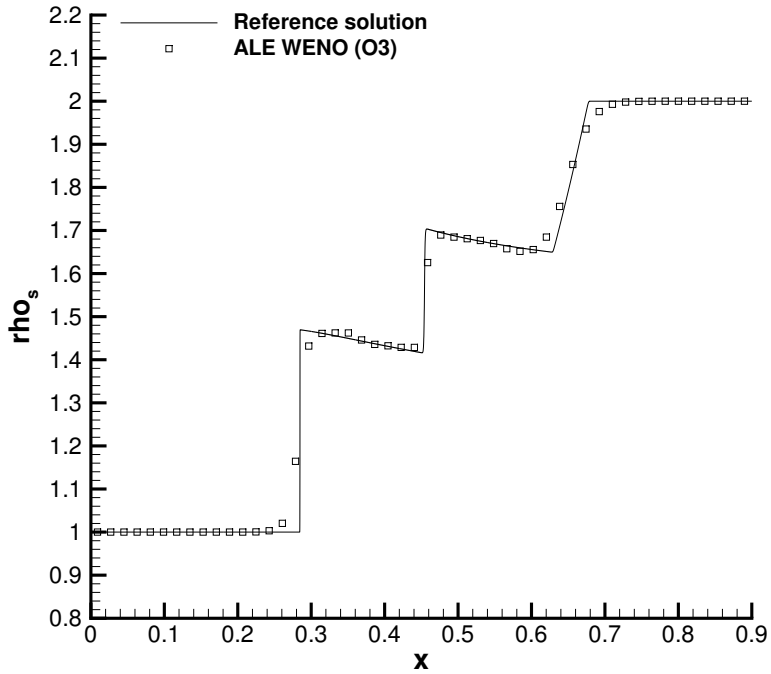

3^{rd} order accurate density distribution for the explosion problem EP1.

Explosion problems

EP2

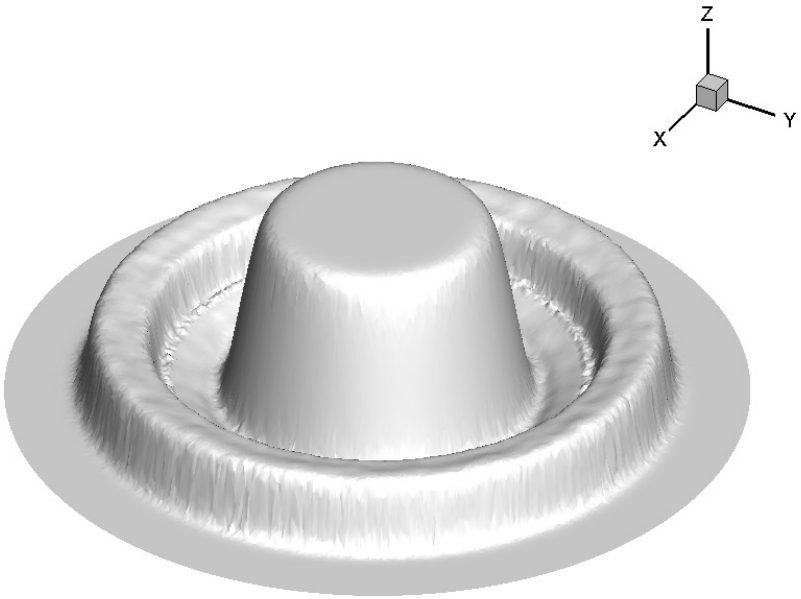

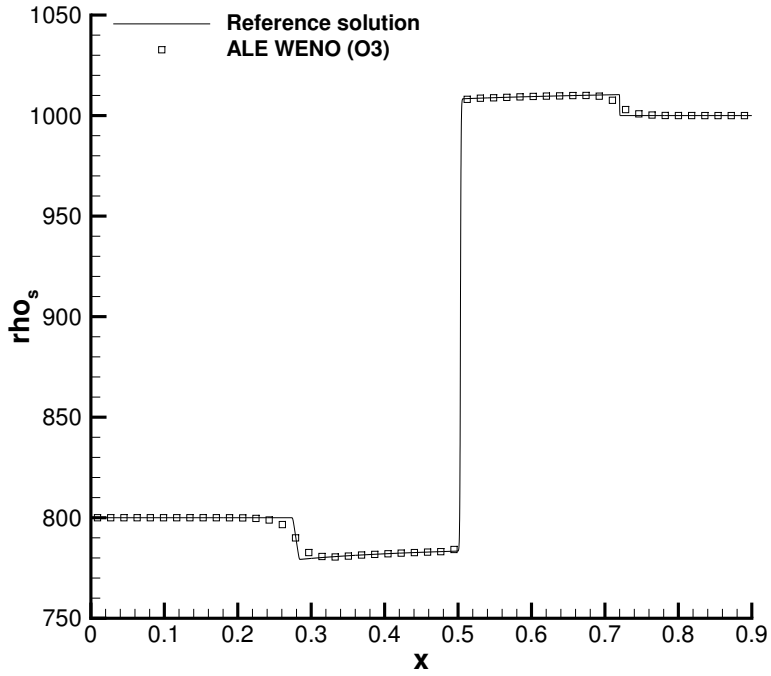

3^{rd} order accurate density distribution for the explosion problem EP2.

Conclusions and Outlook

Conclusions

- we showed high order ALE WENO FV schemes on tetrahedral meshes;
- two different node solvers have been used;
- application to nonconservative hyperbolic balance laws with stiff source terms.

Conclusions and Outlook

Conclusions

- we showed high order ALE WENO FV schemes on tetrahedral meshes;
- two different node solvers have been used;
- application to nonconservative hyperbolic balance laws with stiff source terms.

Outlook

- extension to moving curved elements;
- extension to high order DG direct ALE schemes;
- application to free surface flows.

Thank you!

walter.boscheri@unitn.it

[1] W. Boscheri and M. Dumbser

Arbitrary–Lagrangian–Eulerian One–Step WENO Finite Volume Schemes on Unstructured Triangular Meshes. *Communications in Computational Physics*, 14: 1174-1206, 2013.

[2] M. Dumbser and W. Boscheri

High-order unstructured Lagrangian one–step WENO finite volume schemes for non–conservative hyperbolic systems: Applications to compressible multi–phase flows. *Computers and Fluids*, 86: 405-432, 2013.

[3] W. Boscheri and M. Dumbser

A Direct Arbitrary-Lagrangian-Eulerian ADER-WENO Finite Volume Scheme on Unstructured Tetrahedral Meshes for Conservative and Nonconservative Hyperbolic Systems in 3D. *Journal of Computational Physics*, 275: 484-523, 2014.